HOSTED BY

ELSEVIER

Available online at www.sciencedirect.com

ScienceDirect

Journal of Sport and Health Science

Original article

Decorin, an exercise-induced secretory protein, is associated with improved prognosis in breast cancer patients but does not mediate anti-tumorigenic tissue crosstalk in mice

Marit Hjorth [a,b,†], Casey L. Egan [c,†], Guilherme D. Telles [c,d,e,†], Martin Pal [b,f], David Gallego-Ortega [g], Oliver K. Fuller [c], Emma D. McLennan [c], Ryan D. Gillis [c], Tae Gyu Oh [h,i], George E.O. Muscat [i], Surafel Tegegne [c], Michael S.M. Mah [c], Joanna Skhinas [b], Emma Estevez [b], Timothy E. Adams [j], Matthew J. McKay [k,l], Mark Molloy [k,l], Kevin I. Watt [m,n], Hongwei Qian [n], Paul Gregorevic [n], Thomas R. Cox [b], Pernille Hojman [o,‡], Julie Midtgaard [o], Jesper F. Christensen [o], Martin Friedrichsen [p], Renato V. Iozzo [q], Erica K. Sloan [c], Brian G. Drew [r], Jørgen F.P. Wojtaszewski [p], Martin Whitham [s,*], Mark A. Febbraio [c,*]

[a] *Department of Nutrition, Institute of Basic Medical Sciences, Faculty of Medicine, University of Oslo, Oslo 0317, Norway*
[b] *Garvan Institute of Medical Research, Sydney, NSW 2010, Australia*
[c] *Drug Discovery Biology, Monash Institute of Pharmaceutical Sciences, Monash University, Melbourne, VIC 3052, Australia*
[d] *Laboratory of Neuromuscular Adaptations to Strength Training, School of Physical Education and Sport, University of São Paulo (USP), São Paulo 05508-030, Brazil*
[e] *Center of Study in Exercise and Oncology (CEEO), Campinas 13083-888, Brazil*
[f] *School of Dentistry & Medical Sciences, Charles Sturt University, Wagga Wagga, NSW 2678, Australia*
[g] *School of Biomedical Engineering, University of Technology, Sydney, NSW 2678, Australia*
[h] *College of Medicine, University of Oklahoma, Oklahoma City, OK 73117, USA*
[i] *Institute of Molecular Biosciences, University of Queensland, St. Lucia, QLD 4072, Australia*
[j] *CSIRO Manufacturing, Clayton, VIC 3168, Australia*
[k] *Australian Proteome Analysis Facility, Macquarie University, Sydney, NSW 2109, Australia*
[l] *School of Medical Sciences, University of Sydney, Sydney, NSW 2050, Australia*
[m] *Murdoch Children's Research Institute, The Royal Children's Hospital, Melbourne, VIC 3053, Australia*
[n] *Department of Physiology, The University of Melbourne, Melbourne, VIC 3052, Australia*
[o] *Copenhagen University Hospital, Copenhagen 2100, Denmark*
[p] *Department of Nutrition, Exercise and Sports, University of Copenhagen, Copenhagen 2100, Denmark*
[q] *Sidney Kimmel Medical College, Thomas Jefferson University, Philadelphia, PA 19144, USA*
[r] *Baker Heart and Diabetes Institute, Prahran, VIC 3004, Australia*
[s] *School of Sport, Exercise and Rehabilitation Sciences, University of Birmingham, Edgbaston B15 2TT, UK*

Received 27 February 2024; revised 19 July 2024; accepted 8 August 2024
Available online 26 September 2024

Abstract

Purpose: Regular exercise can reduce incidence and progression of breast cancer, but the mechanisms for such effects are not fully understood. The purpose of this study was to examine the mechanisms behind the protective effects of exercise.
Methods: We used a variety of rodent and human experimental model systems to determine whether exercise training can reduce tumor burden in breast cancer and to identify mechanism associated with any exercise training effects on tumor burden.

Peer review under responsibility of Shanghai University of Sport.
* Corresponding authors.
E-mail addresses: M.Whitham@bham.ac.uk (M. Whitham), mark.febbraio@monash.edu (M.A. Febbraio).
† These three authors contributed equally to this work.
‡ deceased

https://doi.org/10.1016/j.jshs.2024.100991
Cite this article: Hjorth M, et al. Decorin, an exercise-induced secretory protein, is associated with improved prognosis in breast cancer patients but does not mediate anti-tumorigenic tissue crosstalk in mice, *J Sport Health Sci* 2025;14:100991

Results: We show that voluntary wheel running slows tumor development in the mammary specific polyomavirus middle T antigen overexpression (MMTV-PyMT) mouse model of breast cancer but only when mice are not housed alone. We identify the proteoglycan decorin as a contraction-induced secretory factor that systemically increases in patients with breast cancer immediately following exercise. Moreover, high expression of decorin in tumors is associated with improved prognosis in patients, while treatment of breast cancer cells *in vitro* with decorin reduces cell proliferation. Notwithstanding, when we overexpressed decorin in murine muscle or injected recombinant decorin systemically into mouse models of breast cancer, elevated plasma decorin concentrations did not result in higher tumor decorin levels and tumor burden was not improved.

Conclusion: Exercise training is anti-tumorigenic in a mouse model of luminal breast cancer, but the effect is abrogated by social isolation. The proteoglycan decorin is an exercise-induced secretory protein, and tumor decorin levels are positively associated with improved prognosis in patients. The hypothesis that elevated plasma decorin is a mechanism by which exercise training improves breast cancer progression in humans is not, however, supported by our pre-clinical data since elevated circulating decorin did not increase tumor decorin levels in these models.

Keywords: Breast cancer; Exercise training; Muscle secretory factors; Proteoglycans

1. Introduction

Breast cancer is one of the most commonly diagnosed cancers and the leading cause of both cancer death and disability adjusted life-years in women.[1] Improvements in diagnosis and treatment over the past 25 years has, however, seen a marked increased breast cancer survival, with many women recovering to have a normal life expectancy.[2] Epidemiological studies have demonstrated that physical activity can reduce the risk of breast cancer[3,4] and substantially reduce mortality and recurrence in breast cancer patients.[5,6] The evidence showing reduced cancer occurrence with increasing physical activity dates back to the mid-1980s,[7] but the first pre-clinical study showing that exercise inhibits tumor growth dates back to the 1940s.[8] The anti-tumorigenic effects of exercise are mediated by many different mechanisms,[9] including changes in the hormonal milieu,[10,11] decreased fat mass,[12] and immunological changes to the tumor microenvironment.[13] Circulating factors that are secreted from muscle during exercise, so called "myokines", may also contribute to the protective effects.[9] The most well described myokine linked to breast cancer progression is interlukin-6 (IL-6).[9] Plasma concentrations of IL-6 can increase ~100-fold after an acute bout of exercise,[14] and a link between the exercise-induced increase in IL-6 and tumor growth inhibition across various cancer models, including breast cancer, is clear.[15] Other myokines that are suggested to have indirect or direct effects on cancer growth include IL-15 for pancreatic cancer,[16,17] brain derived neurotropic factor[18] and secreted protein acidic and cysteine rich (SPARC) for colon cancer,[19] and Oncostatin M[20] and irisin for breast cancer.[21]

We systematically evaluated the role of exercise training in breast cancer progression and sought to discover whether myokines play a role in any potential protective effect by employing a variety of rodent and human experimental model systems. The models were aimed at determining whether exercise training can reduce tumor burden in breast cancer and identifying mechanisms associated with possible exercise training effects on tumor burden. In initial experiments we identified decorin as a myokine released from the exercising limb, which agrees with other studies describing decorin as an exercise-responsive secretory protein.[22] Decorin is a small proteoglycan in the extracellular matrix of different tissues, with an important role in collagen fiber formation.[23] Decorin has been reported to influence growth factor signaling, proliferation, fibrosis, and vascularization.[24–26] Several preclinical xenograft studies have demonstrated that decorin can slow tumor growth, either by systemic administration[27] or by distant or local overexpression.[28] Furthermore, decorin has been found to have anti-metastatic effects in breast cancer models.[29–31] We therefore conducted several studies in mice to determine whether decorin is an exercise-responsive myokine capable of influencing breast cancer development.

2. Methods

2.1. Human investigations

2.1.1. Human breast cancer datasets

We examined the mRNA expression of decorin in publicly available datasets (GSE11121, GSE4922, GSE7390, and GSE25307) from 4 different breast cancer cohorts.[32–35] Expression and grade information was curated from the National Center for Biotechnology Information (NCBI) database using ShinyGEO,[36] which is a web-based application for analyzing and visualizing Gene Expression Omnibus (GEO) datasets. Expression of non-graded samples were excluded. For survival analyses, we utilized the KMplotter (https://kmplot.com/analysis/), which is an online tool and database containing gene expression data from GEO, The Cancer Genome Atlas Program (TCGA), and the European genome–phenome archive (EGA) repositories.[37] In the KMplotter, we performed analyses on relapse-free survival and distant metastasis-free survival, utilizing data from 3951 to 1746 patients, respectively. Follow-up time was set to 120 months, and we compared patients with high and low decorin expression, split by median expression.

2.1.2. Human arteriovenous exercise study

Healthy men ($n = 12$) were recruited after written informed consent. Participant characteristics were as follows (mean ± standard error of the mean (SEM)): age = 27 ± 1 years, body mass index = 23.9 ± 0.6 kg/m^2, body fat = 21% ± 1%, fasting plasma glucose = 99 ± 2 mg/dL, maximal oxygen consumption (VO_{2max}) = 46.2 ± 1.8 mL/kg/min. The study was approved by the regional ethics committee in Denmark

(Journal number H-3-2012-140) in accordance with the Declaration of Helsinki II. The participants were catheterized in the femoral artery and vein and performed stationary bicycle exercise at increasing intensities (30 min at 55% of VO_{2max}, 20 min at 70% VO_{2max}, and until exhaustion (∼10 min) at 80% of VO_{2max}), as previously described.[38] Arterial and venous blood samples were obtained at baseline, immediately after exercise, and after 4 h of recovery. Blood was obtained in heparinized syringes and mixed with 30 μL 200 mM ethylenediaminetetraacetic acid (EDTA) (Sigma-Aldrich, St Louis, MO, USA) per 1500 μL blood. Blood was centrifuged at 15,000 *g* for 2 min. Leg blood flow was measured using ultrasound techniques (a 9-3 MHz linear array transducer in Power Doppler mode) during rest, as previously described,[39] and estimated during exercise using the formula proposed by Jorfeldt and Wahren.[40] Plasma was diluted 1:1 in phosphate-buffered saline (PBS) (Thermo-Fisher, Scoresby, Australia) and subjected to high-speed centrifugation for isolation of extracellular vesicles (EV), as previously described.[41] The concentration of decorin was measured in EV-free plasma with enzyme linked immunosorbent assay (ELISA) (DuoSet, Cat# DY143; R&D Systems, Minneapolis, MN, USA).

2.1.3. Six-month training intervention study in breast cancer patients

Plasma decorin was measured in a subset of samples from the "Physical Activity after Cancer Treatment" (PACT) trial (ClinicalTrials.gov identifier: NCT00717717), as described in detail elsewhere.[42] The study included 214 cancer survivors (83% female and 17% male) who were randomized to either a health evaluation program or a 12-month rehabilitation program consisting of counseling and high-intensity, group-based exercise training once a week. The overall goal of the physical activity group was ≥3 h/week regular exercise. The supervised training included group-based high-intensity interval training and resistance exercise (approximately 90 min/session) once per week. The high-intensity interval training was on a stationary cycle, with intervals ranging from 30 s (maximum intensity) to 6 min (90−95% of maximum heart rate (HR_{max})) at an exercise to recovery ratio of 1:2 and 3:1, respectively. Resistance training consisted of leg press, chest press, pull down, abdominal crunch, lower back extension, and knee extension and involved 3 sets of 8−10 repetitions at 70%−90% of 1 repetition maximum.

In this study, we utilized samples from 37 patients diagnosed with operable Stages I−III breast cancer (n = 37). Around 70% of the patients received endocrine hormone therapy (Tamoxifen).[43] Decorin was measured in plasma at baseline and after 6 months of counseling and physical activity (DuoSet, Cat# DY143 ; R&D Systems).

2.1.4. Acute exercise in breast cancer patients

Female breast cancer patients (n = 20) were recruited from the Body and Cancer program at Copenhagen University Hospital.[44] The program was a 6-week exercise program for all cancer patients undergoing chemotherapy, consisting of group-based, supervised training sessions with multi-modal high- and low-intensity exercise. These sessions consisted of 90 min of high-intensity training followed by 30 min of relaxation training (3 days per week) and 90 min of body awareness training followed by 30 min of relaxation training (1 day per week). The high-intensity training sessions consisted of a 30-min warmup, 45 min of resistance training (leg press, chest press, pull down, abdominal crunch, lower back or knee extension; 3 series of 5−8 repetitions at 70%−100% of 1 repetition maximum), and 15 min of cardiovascular training (interval training on stationary bicycles at 85%−95% of HR_{max}). In total, the intervention consisted of activities equivalent to 43 metabolic equivalent of task (MET) hours per week. More details on the intervention are published elsewhere.[44]

The subjects recruited to the acute exercise study fulfilled the same inclusion criteria as the PACT study but were on adjuvant chemotherapy. The participants were at least 7 days from the last dose of chemotherapy. The acute exercise session was a part of the Body and Cancer Program (described in detail[44]), which took place halfway through the 6-week program and consisted of a 30-min warmup, 60 min of whole body resistance training, and 30 min of high-intensity aerobic exercise (pulse > 80%HR_{max}) on stationary bicycles. The average workload was approximately 70% of maximal heart rate for the whole session. The participants fasted for at least 2 h before the exercise session. Blood samples were collected before and immediately after the exercise bout.

2.2. Experiments in mice

Experiments were approved by the Alfred Medical Research Education Precinct, Garvan Institute/St. Vincent's and/or Monash Animal Ethics Committees, in accordance with the Australian code for the care and use of animals for scientific purposes. The *in situ* decellularization of tissues (ISDoT) experiments were approved by the Danish Inspectorate for Animal Experimentation. Friend Virus B NIH Jackson Mammary specific polyomavirus middle T antigen overexpression (FVB/NJ MMTV-PyMT) mice were originally created by Guy et al.[45] as previously described. MMTV-PyMT mice with a C57BL/6J genetic background were supplied by the University of California, San Diego. MMTV-PyMT mice were bred by crossing heterozygous $PyMT^{(tg/+)}$ male mice with female wide type (WT) mice to produce $PyMT^{(tg/+)}$ and WT littermates for experiments. Mice were housed in a 12 h:12 h light:dark cycle with 2−5 animals per cage. All experiments commenced when mice were 6 weeks of age unless otherwise stated, and all mice were fed a standard chow diet ad libitum and with free access to water. At termination, animals were anesthetized by 4% isoflurane (Provet, Victoria, Australia) at a rate of 1 L/min. Blood was collected by cardiac puncture, which was followed by cervical dislocation. Tissues were collected and snap frozen in liquid nitrogen or processed for microtomy.

2.2.1. Exercise training study in the FVB/NJ MMTV-PyMT mouse model

Treadmill exercise: Female MMTV-PyMT/FVB-WT (tumor-free) animals of 16−17 weeks of age were placed into 2 groups. One group remained sedentary and the other were

familiarized to a motorized treadmill 3 times on separate days. The animals were subsequently fasted for 4 h, and subjected to 90 min of treadmill running, starting at a speed of 4 m/min and increasing by increments of 2 m/min every 10 min until reaching 24 m/min. Blood was collected with cardiac puncture immediately after the run. Decorin concentration in serum samples was measured with an ELISA kit (DuoSet, Cat# DY1060; R&D Systems.

For the wheel running experiment, mice were either housed alone with running wheels or in pairs in home cages with 2 locked or 2 functional running wheels (Columbus Instruments, Columbus, OH, USA) (Supplementary Fig. 1A). The surface area of tumors in all mammary glands was measured twice per week with callipers. Animals were euthanized when they reached the ethical endpoint, which was defined as having a tumor burden of 10% ± 3%. Approximate tumor burden was estimated from total tumor surface area. All tumors were later dissected and weighed for accurate determination of total tumor burden.

2.2.2. Treadmill running and quantitative proteomic profiling

Generation of Stable isotope labeling using amino acids in cell culture (SILAC) mice: Male and female C57BL/6J mice of 8 weeks of age were selected for SILAC labeling to create a tissue bank for spike-in or pulse-chase quantitative proteomics. Breeding pairs where fed ad libitum on custom $^{13}C_6$ Lysine chow (MouseExpress L-Lysine $^{13}C_6$, 99%, Cambridge isotopes MLK- LYS-C, Tewksbury, MA, USA), and resultant litters were paired again for F3 offspring to allow full incorporation of the lysine label into the mouse proteome as confirmed by mass spectrometry. For treadmill exercise, 8-week-old male C57BL/6J mice ($n = 3$ per group) were randomly assigned to treatment groups (Exercise or Rest). Exercising animals carried out a 90-min treadmill running protocol, starting with a speed of 4 m/min and increasing by increments of 2 m/min every 10 min until reaching 24 m/min, while resting controls were placed on the motionless treadmill for the same duration. After euthanasia, the gastrocnemius muscle was dissected, homogenized in lysis buffer (50 mM TRIS (pH = 7.5), 1 mM EDTA, 150 mM NaCl, 0.1% sodium deoxycholate, 1% NP-40, 1× protease inhibitor cocktail (Sigma-Aldrich) and combined at a 1:1 ratio with a mixed muscle homogenate processed from the fully labeled $^{13}CLys_6$ SILAC mice. Lysates were fractionated via 1D sodium dodecyl sulfate-polyacrylamide gel electrophoresis (SDS PAGE) and cut into 10 sections, washed, and rehydrated in 100 mM ammonium bicarbonate before reduction and alkylation in 10 mM dithiolthretol and 25 mM Iodoacetamide, respectively. Digestion was carried out in either LysC or trypsin with the resultant peptides dried and resuspended in 2% acetonitrile, 0.1% formic acid. Data from samples were then acquired via LC/MS−MS on an Orbitrap Elite (Thermo Fisher Scientific, Waltham, MA, USA) using a top 15 method with collision-induced disassociation (CID) fragmentation. Raw data were searched using Mascot (Matrix Science, London, UK) through the Proteome Discoverer software (Thermo Fisher Scientific) against the Mus Musculus Swissprot database. Search conditions included dynamic modifications for methionine (oxidation) and indicated quantification using SILAC (Lys6). Searches were performed using either trypsin or LysC as the enzyme, and mean H/L was calculated for each protein and expressed as a ratio of ratios (Exercise or Rest). Processed quantitative proteomics data are freely available at https://doi.org/10.25500/edata.bham.00001030.

2.2.3. ISDoT: In situ decellularization of tissues for proteomic analysis

Primary tumors and metastatic lymph nodes were from a breast cancer model in which 4T1 cells were orthotopically implanted in the third thoracic mammary fat pad of 8-week-old female BALB/c mice (Taconic Biosciences, Germantown, NY, USA), as described in detail previously.[46] Mice were prepared for the ISDoT procedure after 21 days, when the primary tumors reached a maximum of 10 mm in diameter. Lung metastases were from mice that were implanted with 4T1 cells into the inguinal fat pad, as described previously.[46] When the primary tumors reached a diameter of 10 mm, they were excised under general anesthesia. ISDoT was performed when mice had developed lung metastases. The ISDoT procedure involves decellularization of whole organs, leaving native extracellular matrix (ECM) structures intact. The procedure has been described in detail, accompanied by an instructional video.[46] The procedure involves surgical modification of vascular flow, followed by perfusion of catheterized organs with detergents.

For proteomics analyses, organs were then solubilized in urea buffer. Proteins were reduced, alkylated, deglycolsylated, and digested with LysC and trypsin. Peptides were acidified, desalted on packed C18 StageTips, and concentrated on an Eppendorf Speedvac (Hamburg, Germany), as described in detail.[47] Each sample was run unfractionated on a Thermo Fisher Q-Exactive Mass Spectrometer. Raw MS/MS spectra were processed using MaxQuant software (Max Plank Institute, Munich, Germany), as described.[46]

2.2.4. Overexpression of decorin in skeletal muscle

Recombinant adeno-associated virus (AAV) serotype 6 was generated as previously described,[48] with plasmids (GenScript Biotech, Piscataway, NJ, USA) containing a decorin construct with a C-terminal FLAG tag under the control of a cytomegalovirus (CMV) promoter (AAV:Dcn) or a noncoding control vector (AAV:Con). Intramuscular administration was done by injecting 1×10^{12} vector genomes in both hind legs as follows. At 6 weeks of age, animals were anesthetized with isoflurane at a rate of 1 L/min of 4% isoflurane (Provet) for induction and 1 L/min of 2% isoflurane for maintenance. Animals were given a subcutaneous dose of ketoprofen (Zoetis, Parsipanny, NJ, USA). Hind legs were shaved, and tibialis anterior, gastrocnemius, and quadriceps muscles were injected with 30 μL rAAV diluted in PBS. As a negative control for decorin, we used muscle from decorin-deficient ($Dcn^{-/-}$) animals.

2.2.5. Recombinant decorin injection experiment in mice

Female severe combined immunodeficiency disease (SCID) mice were obtained from the Animal Research Center (Perth, Australia) from 6 to 8 weeks of age and housed at the animal

holding facility for a period of 1 week before being enrolled into the experimental study. All mice remained on a normal chow diet and were weighed twice a week for the duration of the study. We performed 2 separate experiments. In the first experiment (low dose), mice were injected with the epithelial human breast cancer cell line MDA-MB-231-HM into the 4th left mammary pad at the commencement of the experiment. Following this, tumor and metastasis progression were monitored via caliper of primary tumors and bioluminescence imaging measurements, respectively. Twenty-six to 30 days later, animals underwent cardiac puncture followed by cervical dislocation, and tissues were harvested for analysis. After 12−16 days (∼14 days) post tumor-cell inoculation, mice were injected with 100 μg of recombinant decorin or an equal volume of saline (Control) every second day into the intraperitoneal (IP) space for the remainder of the experiment. As results from this first experiment suggested that we may have insufficiently dosed the animal with recombinant decorin, we performed an additional (high dose) experiment. The protocol was similar to the first experiment except for a few changes. Treatment commenced ∼7 days post tumor-cell inoculation, and animals were dosed daily with 10 mg/kg body weight (∼2.5 times the dose of Experiment 1). Recombinant decorin was purified by Commonwealth Scientific and Industrial Research Organisation (CSIRO) (Melbourne, Australia) using human embryonic kidney 293F (HEK293F) cells. Affinity purification strategy used HisTrap Excel (Cytiva, Mount Waverley, VIC, Australia) and size exclusion chromatography column Superdex 200 26/60 (Cytiva).

2.2.6. Single cell RNA sequencing (RNAseq)

Mammary tumors were collected from MMTV-PyMT/FVB mice at 14 weeks of age, digested to a single cell suspension, sorted by Fluorescence-activated cell sorting (FACS), and subjected to Drop-seq as previously described[49] following standard recommendations.[50] Dead cells were removed by labeling with Annexin-specific magnetic beads cell isolation (MACS) beads and an autoMACS® Pro separator (Miltenyi, Bergisch Gladbach, Germany). Cell preparations with high viability (>85% viability assessed by FACS) were loaded into the microfluidic Drop-seq pipeline. Cells were captured using the microfluidic devices described for Drop-seq[51] following the online protocol Version 3.1 (www.mccarrolllab.com/dropseq). The cDNA libraries were sequenced in Nextseq 500 using Nextseq 500 High Output v.2 kit (75 cycles, Cat# FC-404-2005; Illumina, San Diego, CA, USA) following the recommendations of Macosko et al.[51] with a few modifications, as previously decribed.[49] A total of approximately 3000 cells were sequenced per run. Bioinformatics analyses were performed as previously described.[49] The dataset from Valdes-Mora et al.[49] was reanalyzed with data from MMTV-PyMT (WT) tumors only. Downstream analyses were performed in Seurat (v Seurat 3)[52] using a total of 8336 cells from 8 MMTV-PyMT tumors (minimum 400 genes per cell barcode, <5% mitochondrial genes, <8000 molecules/cell). We performed a Shared Nearest Neighbor (SNN) clustering analysis calculating k-nearest neighbors (Jaccard Index) using 30 principal components, followed by differential expression analysis and uniform manifold approximation and projection dimensional reduction projection.[53]

2.2.7. Histology and immunofluorescence staining

Lungs were fixed in 10% phosphate-buffered formalin, embedded in paraffin, sectioned, and stained with haematoxylin and eosin for routine histology. Sections of whole lungs were scanned with a 5× lens on a Leica DM 6000 Power Mosaic microscope (Leica Camera; Wetzlar, Germany) with a stepping stage for mosaic image acquisition. Numbers of metastases were manually counted with ImageJ software (National Institutes of Health, Bethesda, MD, USA). Tumor tissue was embedded in optimal cutting temperature (O.C.T.™) Compound (Tissue-Tek®, Qiagen, Germantown, MD, USA)) and frozen in liquid nitrogen cooled isopentane. Tissues were then cryosectioned onto superfrost glass slides, fixed in 4% paraformaldehyde, blocked in 1% horse serum, and incubated with primary antibodies (decorin; R&D Systems #AF1060; and Collagen 1A,#Sc-59772, Santa Cruz Biotechnology, Dallas, TX, USA) in 1% bovine serum albumin, 1% horse serum, 0.01% sodium azide, and 0.03% triton X-100 in PBS overnight. The slides were then incubated with DAPI and Cy™3 and Alexa Fluor®488-conjugated secondary antibodies (Jackson ImmunoResearch; West Grove, PA, USA). Image acquisition was done on a Leica DM5500 microscope.

2.2.8. Immunoprecipitation and immunoblotting

Tissues (m. gastrocnemius, mammary tumor tissue, and mammary fat pad) were lysed and homogenized in lysis buffer (50 mM Tris, 130 mM NaCl, 5 mM EDTA, 1%Tween20, 1 mM PMFS, and 10 mM NaF). Samples with equal amounts of protein (2.5 mg) or a protein free, negative control (C−) were loaded on to anti-FLAG M2 Magnetic beads (Cat# M8823; Sigma-Aldrich) according to manufacturer's instructions. After incubation and washing, samples were eluted in 20 μL Laemmli buffer, and separated on Criterion TGX™ gels (Bio-Rad Laboratories, Hercules, CA, USA). Proteins were transferred to nitrocellulose membranes (Bio-Rad Laboratories) using the Trans-Blot Turbo transfer system and RTA transfer kit (Bio-Rad, South Granville, NSW, Australia). Membranes were blocked in Tris buffered saline containing 0.1% Tween-20 (TBS-T) and 5% bovine serum albumin (BSA) and incubated over night with primary antibodies (decorin, LF-114 antisera from Fisher et al.,[54] and FLAG, Cat#14793; Cell Signaling Technology, Danvers, MA, USA). After washing, membranes were incubated with appropriate HRP-conjugated, confirmation specific, secondary antibodies. The ChemiDoc™ Touch Imaging System (Bio-Rad) was used for chemiluminescence detection.

2.2.9. Western blot

Tumor protein concentration was quantified using a Pierce BCA protein assay kit (Thermo Fisher). Two AAV:Dcn gastrocnemius lysates from the overexpression experiments were used as positive controls. Then, 20 μg of protein was diluted in Laemmli buffer (Bio-Rad) and loaded into each

well. Proteins were separated using 10% SDS-PAGE on polyacrylamide gels, transferred to membranes (Trans-Blot Turbo System, Mixed MW 7-min protocol; Bio-Rad), and blocked with 5% BSA. After addition of primary antibodies, membranes were incubated overnight at 4˚C, followed by 60 min of incubation with secondary antibodies and detection using Pierce ECL/Super ECL detection reagent (Thermo Fisher) on the ChemiDoc Gel Imaging System (Bio-Rad). The primary antibody used was decorin (GTX101250; GeneTex, Irvine, CA, USA). The secondary antibody used was goat anti-rabbit (7074; Cell Signaling Technology). Decorin protein levels were calculated using total protein normalization.

2.3. In vitro experiments

2.3.1. Breast cancer cell proliferation assay

For breast cancer cell proliferation studies, breast cancer cells (MCF7 and T47D) were plated into 24-well culture plates at a density of 20,000 cells per well and allowed to attach overnight before the medium was replaced with the addition of decorin at specified doses (1 nM and 10 nM) or left blank (no treatment). After 48 h, cells were washed twice with PBS and stained for 15 min in Hoechst nuclear dye (Invitrogen, Waltham, MA, USA). Cell number was estimated by plotting Hoechst fluorescence measured in each well as determined using an Enspire Plate Reader (Perkin Elmer, Waltham, MA, USA) against a pre-determined standard curve.[55]

2.4. Statistics

Group differences were tested with Student's *t* tests for paired or unpaired observations or with Mann-Whitney test unless otherwise stated. A p value <0.05 was determined significant. To test for group differences when having repeated measures, we used a repeated measures, two-way Analysis of varoiance (ANOVA) or mixed effects model (Graphpad Prism v.8 and v.9; La Jolla, CA, USA). Comparison of survival of breast cancer mice was done with Mantel−Cox test.

3. Results

3.1. The suppression of tumor development in MMTV-PyMT mice by exercise is abrogated by singly housing mice

The MMTV-PyMT is a pre-clinical model of mammary cancer, which progresses through hyperplasia to cancer before losing estrogen receptor expression and metastasizing to lungs.[56] To investigate whether exercise slows breast cancer development in mice, MMTV-PyMT (FVB/N background) mice were housed with either functional (Run) or locked (sedentary (Sed)) running wheels from 6 to 13 weeks of age (Supplementary Fig. 1). In initial experiments, mice were housed alone, and those with functional running wheels ran on average >20,000 revolutions per day (rev/day) (range: 5668−55,578 rev/day), which corresponds to >8 km/day (Supplementary Fig. 2A). Despite the significant daily running in the Run group, there were no differences between Run and Sed mice in terms of body mass, fat mass, spleen mass, or gonadal fat pad mass. As expected, however, total lean mass and muscle mass, as measured by quadriceps weight, was increased in Run compared with Sed animals (Supplementary Fig. 2B−2G). At 11 weeks, neither total tumor nor largest tumor surface area were different when comparing Sed with Run animals (Supplementary Fig. 2H−2I). Furthermore, at the termination of the experiment at 13 weeks, tumor mass (Supplementary Fig. 2J) or the number of lung metastases per microtomy section (Supplementary Fig. 2K) were not different when comparing Run with Sed animals. In a separate cohort, mice were euthanized when tumor burden was 10% ± 3% of body weight. Survival time was not significantly different in Run compared with Sed animals (Supplementary Fig. 2L).

Given the known effects of exercise on tumor development,[15] we were surprised that our exercise intervention had little or no effect on whole body physiology or tumor development. There has been much debate as to whether single housing mice is detrimental or stressful. Mice prefer social contact when given the choice—even male mice that are bullied by more aggressive male companions.[57] It has been speculated that single housing mice makes them less capable of coping with external stressors than their group-housed counterparts.[58] Recently, it was demonstrated that single-housed male mice are negatively affected by isolation and have dysregulated serotonergic signaling activity, a marker of psychological stress.[59] Less research has been conducted in female mice, but a recent study demonstrated single housing mice induces cognitive impairment and depression-like behavior in mice, irrespective of sex.[60] Accordingly, we sought to determine whether housing mice influenced the voluntary wheel-running response to tumor development in the MMTV-PyMT mouse model of mammary cancer by repeating the above experiment while avoiding the confounding stress of social isolation by housing mice in pairs with 2 running wheels per cage (Supplementary Fig.1B). In this experiment, access to functional running wheels had no effect on body mass, gonadal fat pad mass, spleen mass, or lean mass (Fig. 1A−1D). In contrast, however, to the experiment in single housed mice, in this experiment access to functional running wheels decreased fat mass (Fig. 1E). Running also increased muscle mass, as measured by quadriceps weight, compared with Sed animals (Fig. 1F). More importantly, when mice were dually housed, total tumor surface area was reduced (Fig. 1G) and the largest tumor surface area showed a tendency to decrease (Fig. 1H) when comparing Run with Sed. Furthermore, upon termination of the experiment at 12 weeks, tumor mass as a percentage of total body weight was markedly reduced when comparing Run with Sed (Fig. 1I), although the number of lung metastases per section was unaffected by exercise (Fig. 1J). These data suggest that voluntary wheel running can indeed slow breast cancer progression in the MMTV-PyMT mouse model of mammary cancer—but, critically, not when mice are single-housed. We reasoned that stress hormones such as cortisol may, in part, play a role in the differences we observed when comparing single- with dual-housed animals, but we saw no effects on plasma cortisol levels from either exercise or housing (Supplementary Fig. 3).

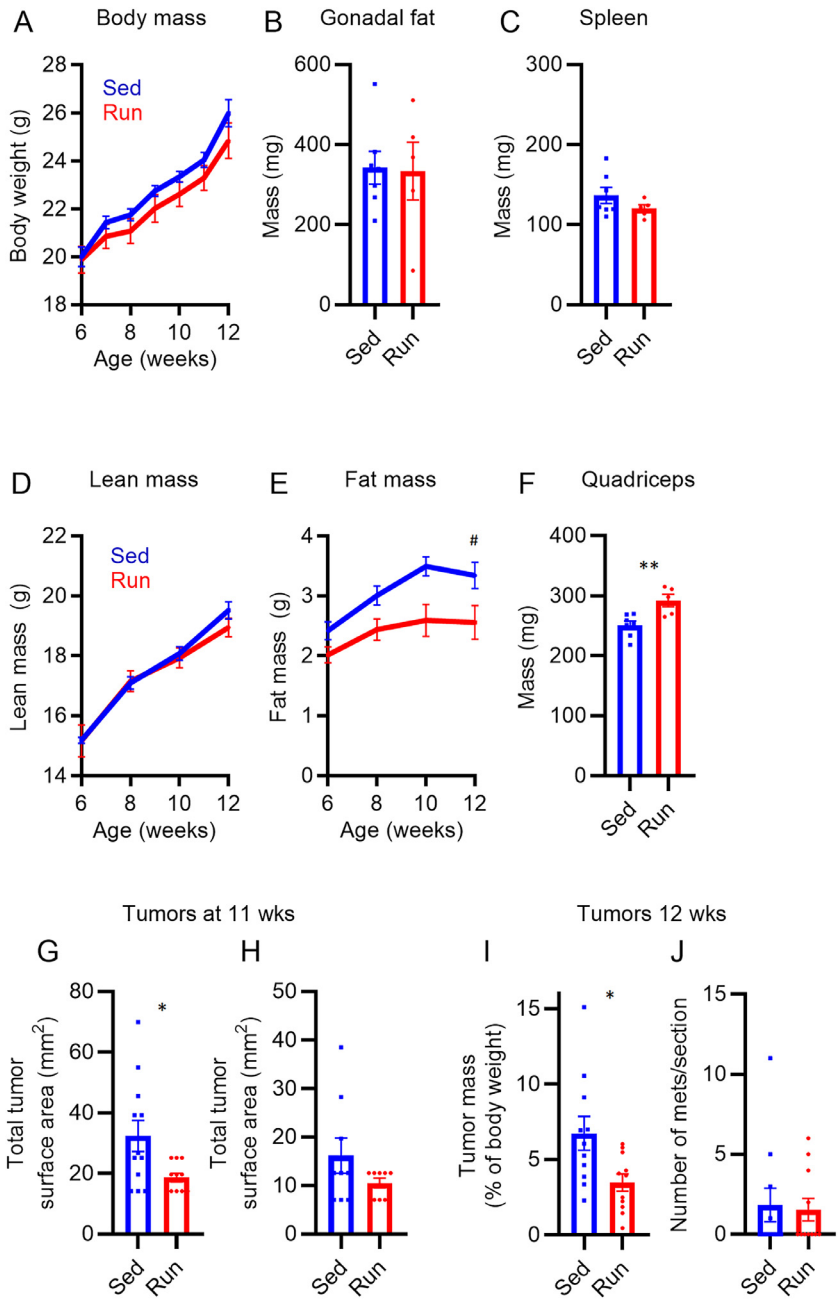

Fig. 1. Voluntary wheel running suppresses tumor growth in dually housed MMTV-PyMT mice. Mice were housed in pairs with 2 running wheels per cage from 6 weeks of age. Wheels were either locked or functional. (A) Body mass, (B and C) gonadal fat mass and spleen mass at termination, (D) lean mass, (E) fat mass, and (F) quadriceps muscle mass at termination, in sedentary (Sed) and running (Run) mice. Tumor burden was estimated by measuring tumor surface area of tumors in (G) all mammary glands and (H) the largest tumor at 11 weeks of age. (I) Tumor burden was measured as total tumor mass relative to body weight (%), and (J) number of lung metastases was quantified as number of metastatic lesions per microtomy section at termination. Statistical testing was done with two-way analyses of variance or mixed effects model for repeated measures or Student's *t* test. * $p < 0.05$, ** $p < 0.01$, between groups; # $p < 0.05$ group × time effect. Data expressed as means ± SEM ($n = 4–11$ mice per group). MMTV-PyMT = mammary specific polyomavirus middle T antigen overexpression mouse model; SEM = standard error of the mean; wks = weeks.

3.2. Decorin is an exercise-induced myokine in mice and humans

To identify exercise-responsive secretory proteins that may play a role in mediating the protective effects of exercise, we performed a quantitative proteomics screen. We first created fully labeled, $^{13}C_6$-Lysine SILAC mice, as previously described.[61] We took muscle (m. gastrocnemius) lysates from 1 non-exercised and 1 treadmill-exercised SILAC mouse as well as from exercised ($n = 3$) or non-exercised ($n = 3$) C57/BL6 mice. We then mixed lysates from the exercised and non-exercised SILAC mice with the exercised and non-exercised C57/Bl6 mice in a 1:1 ratio and analyzed samples by liquid chromatography−tandem mass spectrometry. In total, we detected 2280 proteins, of which 483 proteins were detected in both resting and exercising mice (Fig. 2A).

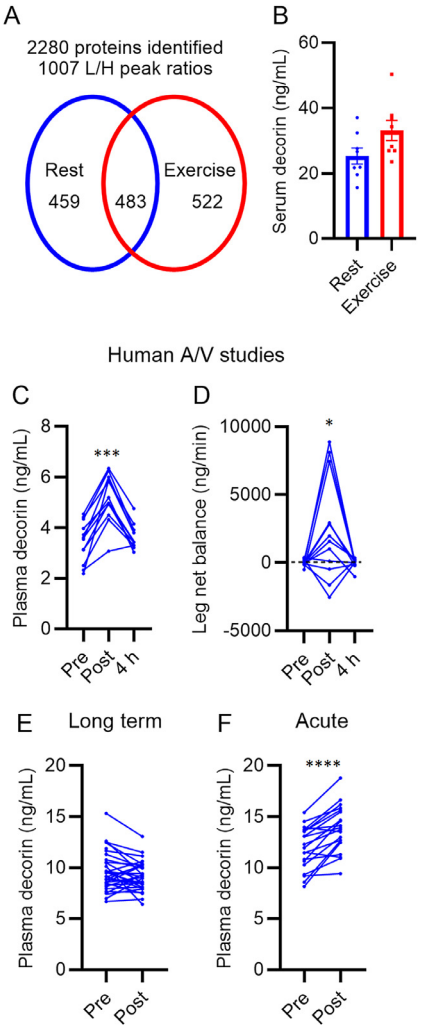

Fig. 2. Decorin is an exercise-induced muscle secretory factor. (A) Male C57Bl/6J mice were acutely exercised on a motorized treadmill for 90 min ($n = 3$) or kept resting in the home cage ($n = 3$). Quantitative proteomic profiling of m. gastrocnemius using a $^{13}C_6$ SILAC labeled reference sample. Number of detected proteins and quantified L/H ratios. (B) Female ($n = 8$ per group), tumor-free MMTV-PyMT-WT mice were exercised on a treadmill for 90 min; Serum decorin immediately after exercise and in resting littermates. (C and D) 12 healthy male participants were catheterized in the femoral artery and vein and subjected to bicycling at increasing intensities for approximately 1 h. Blood samples were taken before (pre), immediately after (post), and after 4 h recovery; (C) Plasma concentration and (D) leg net balance, calculated as arteriovenous difference multiplied by leg blood flow. (E) Plasma decorin in patients ($n = 37$) from the PACT trail. (F) Patients had undergone treatment for operable Stages I–III breast cancer, and plasma decorin was measured before and after 6 months of counseling and exercise training. Plasma decorin in breast cancer patients ($n = 20$) before and after 2 h of acute exercise (high-intensity aerobic training and resistance training). Data are expressed as means ± SEM and include individual data points (B) or are expressed as individual data points (C–E). * $p < 0.05$, *** $p < 0.001$, **** $p < 0.0001$. A/V = arteriovenous difference; L/H = light/heavy label ratio; MMTV-PyMT-WT = the mammary specific polyomavirus middle T antigen overexpression mouse model wild type (tumor free); SEM = standard error of the mean.

We identified several secretory proteins that were increased after exercise, and the top 10 ranked proteins are shown in Table 1. The 6th ranked protein, decorin, was increased by 55% (Table 1). Decorin peaked our interest because, firstly, it has been reported to increase in human serum following exercise[22] and, secondly, because it has been suggested to have a protective effect against breast cancer in preclinical models.[29] To investigate whether decorin is secreted into circulation in our mouse models, we performed another acute exercise study on female FVB/NJ mice. After 90 min of treadmill running, decorin tended to increase in the plasma of exercising mice compared with their resting littermates ($p = 0.06$; Fig. 2B).

Table 1
Secretory proteins increased in murine skeletal muscle after exercise.

Protein name	Expression (mean. H/L)		Ratio Exercise/rest
	Rest	Exercise	
Annexin A2	0.82	3.53	4.29
Complement C3	0.53	1.24	2.36
Alpha-2-macroglobulin	0.80	1.68	2.09
Carboxylesterase 1C	0.49	0.88	1.81
Dehydrogenase/reductase SDR family member 7C	0.54	0.97	1.80
Decorin	0.92	1.42	1.55
ADP-dependent glucokinase	1.25	1.93	1.54
Hemopexin	1.19	1.70	1.43
Cathepsin D	0.56	0.76	1.35
Mimecan	0.91	1.22	1.34

Abbreviations: ADP = adenosine diphosphate; H/L= heavy/light label ratio; SDR = Short-chain dehydrogenase/reductase.

Although proteins can increase in circulation following exercise, they could come from a range of tissues, including the liver, adipose tissue and brain (for review see Ref.[62]). To examine whether decorin is secreted from skeletal muscle in humans, we first quantified decorin in plasma and then determined the net flux of decorin from the contracting limb by performing arterio–venous balance studies in 12 healthy male subjects undertaking 1 h of bicycle ergometer exercise, as previously described.[63] We found that decorin increased in arterial plasma by 60% immediately after the exercise session and returned to baseline after 4 h of recovery (Fig. 2C). Moreover, we detected a significant net release of decorin from the exercising limb immediately following exercise, which also returned to baseline 4 h into recovery (Fig. 2D). These data identify decorin as an exercise-induced secreted protein, most likely coming from skeletal muscle.

Next, we analyzed plasma in a subset of samples from the PACT trial.[43] Women with breast cancer ($n = 37$) underwent a 6-month exercise training study, and after this intervention, blood was collected and plasma analyzed for decorin. Exercise training did not increase plasma decorin at rest (Fig. 2E). We then measured plasma decorin after a 2-h acute exercise bout in breast cancer patients recruited from the Body and Cancer program at Copenhagen University Hospital. Acute exercise increased plasma decorin levels in these breast cancer patients (Fig. 2F). These data identify decorin as a protein that increases in breast cancer patients acutely following exercise.

3.3. Decorin expression in mammary tumors is associated with survival and tumor grade

Decorin has been identified as a tumor-suppressor.[64] To characterize the expression of decorin in mammary tumors, we

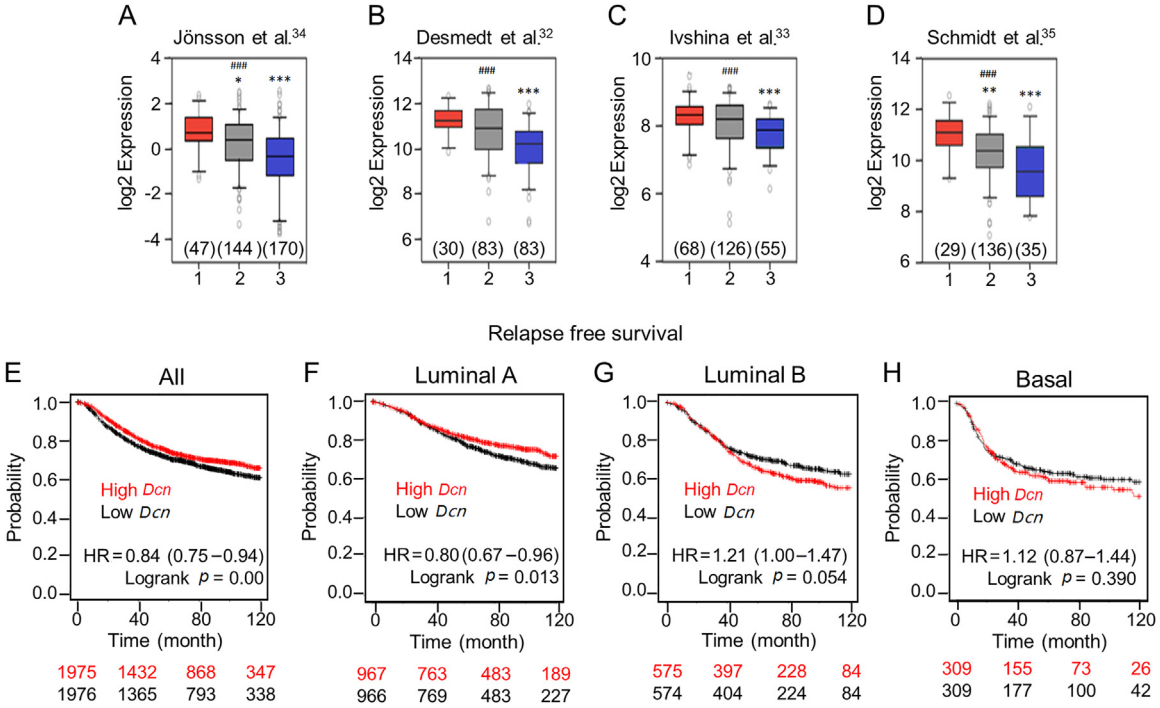

Fig. 3. Expression of decorin in human tumors. Decorin is a prognostic marker in human mammary tumors. (A−D) Decorin mRNA expression in mammary tumors Grades 1−3, from 4 different breast cancer cohorts. Data were extracted using the ShinyGEO application. (E−H) Survival analyses comparing breast cancer patients with high or low tumor expression of decorin. Data were from Kaplan−Meier plotter containing data from several publicly available transcriptomic datasets. The numbers in parenthesis indicate the number of samples in each group. HR, logrankanalysis from Kaplan-Meier plotter. Black and red numbers on the bottom rows indicate the number at risk in the 2 groups (red: high decorin expression and black: low decorin expression). * $p < 0.05$, ** $p < 0.01$, and *** $p < 0.001$ for difference between the indicated group and the reference group (Grade 1). ### $p < 0.001$ for overall difference (Kruskal−Wallis test). Dcn = Decorin; GEO = gene expression omnibus; HR = hazard ratio; KMplot = Kaplan-Meier plot; MMTV-PyMT = the mammary specific polyomavirus middle T antigen overexpression mouse model; MMTV-PyMT/FVB = the mammary specific polyomavirus middle T antigen overexpression mouse model on a Friend Virus B NIH Jackson genetic background.

utilized publicly available datasets from 4 human breast cancer cohorts.[32−35] Tumor decorin expression was inversely associated with tumor grade, with a lower mRNA expression in Grade 3 tumors in all cohorts (Fig. 3A−3D). To further explore the association between decorin and survival, we utilized the KMplotter,[65] which contains data on survival and gene expression from the GEO and EGA repositories. Patients with a high tumor expression of decorin had improved relapse-free survival, with a 16% reduction in hazard ratio in breast cancers overall (Fig. 3E) and a 20% reduction in hazard ratio in luminal A breast cancers (Fig. 3F). Decorin was not associated with survival in luminal B or basal type breast cancers (Fig. 3G and 3H), indicating that decorin may be more important as a tumor suppressor in lower grade tumors.

3.4. Decorin levels are reduced in tumors compared with adjacent non-tumor tissue

We next examined decorin in mammary tumors from MMTV-PyMT mice. Decorin mRNA expression was reduced by >80% in tumors compared with healthy mammary fat pad (Fig. 4A). Immunofluorescence staining of PyMT tumors showed that decorin was expressed in the fibrous cap surrounding the tumor, and that it was co-localized with collagen 1A1 (Fig. 4B). We observed little or no staining for decorin within the tumor lesions, which consist of solid sheets of malignant cells. Next, to characterize decorin in murine breast cancer, we quantified decorin in mammary primary tumors and metastatic lung and lymph nodes from a 4T1 orthotopic model. Tissues were decellularized and subjected to quantitative MS/MS. Decorin abundance was reduced by 60% in mammary tumors compared with healthy mammary tissue (Fig. 4C). There was also a tendency for reduced decorin abundance in metastatic lung (Fig. 4D) but not metastatic lymph nodes (Fig. 4E).

3.5. Decorin is expressed by secretory cancer-associated fibroblasts

To further characterize the expression of decorin in mammary tumors, we performed single-cell RNAseq of MMTV-PyMT tumors. Consistent with previous reports,[49,66] we identified 2 distinct classes of cancer associated fibroblasts (Fig. 5A and Supplementary Fig. 4): scaffolding myofibroblasts and secretory fibroblasts. Decorin was specifically expressed in secretory fibroblasts and was, to a much lesser extent, expressed in the cancer epithelial cell population (Fig. 5B and 5C). Secretory fibroblasts consisted of ECM-remodeling and inflammatory fibroblast subpopulations. ECM fibroblasts had a high expression of structural matrix

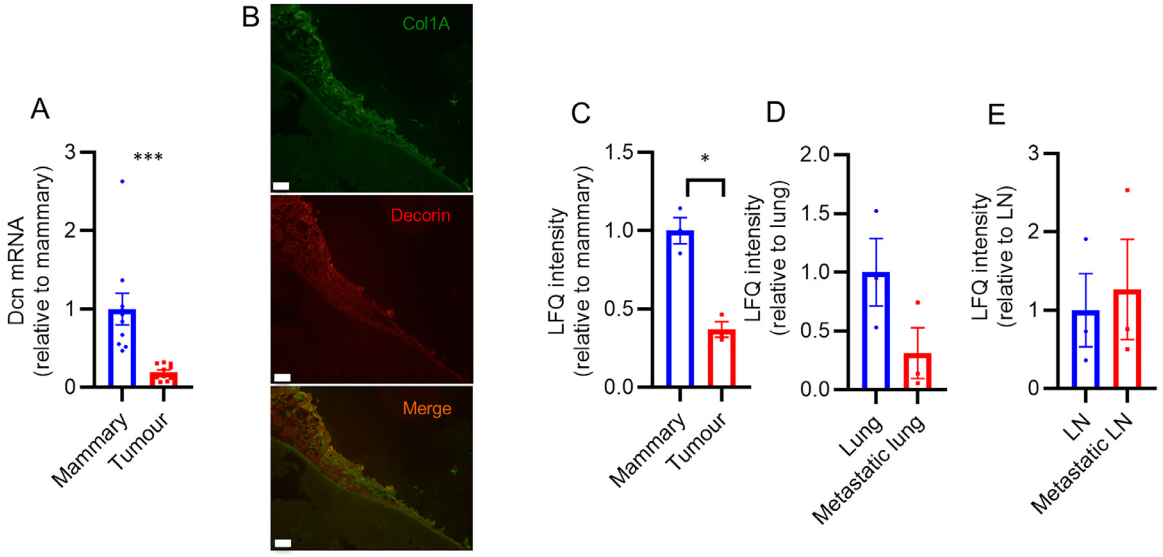

Fig. 4. Expression of decorin in murine tumors. (A) mRNA expression of decorin in MMTV-PyMT tumor and mammary fat pad. (B) Immunostaining of collagen Type I α 1 (Col1a1) and decorin in tumors from MMTV-PyMT/FVB mice. Scale bar represents 100 μm. (C−E) Decorin was quantified with MS/MS in decellularized tissues from BALB/c mice implanted with 4T1 cells ($n = 3$). (C) Primary mammary tumor and healthy mammary fat pad. (D) Healthy and metastatic lung. (E) Healthy and metastatic lymph node. Represented as LFQ intensities relative to healthy tissue. Data are expressed as means ± SEM. * $p < 0.05$, *** $p < 0.001$, Student's t test. Dcn = Decorin; LFQ = label-free quantitation; LN = lymph node; MMTV-PyMT = mammary specific polyomavirus middle T antigen overexpression mouse model.

components (such as collagens and elastin), matricellular proteins, and various enzymes involved in ECM remodeling. Inflammatory fibroblasts also expressed ECM components but had a higher expression of immune factors, including genes involved in cytokine−cytokine receptor interactions and complement factors.[49]

Decorin was highly expressed in both ECM and inflammatory fibroblasts and was co-expressed with biglycan and lumican (Fig. 5D and 5E). These are genes that belong to the same family of Small Leucine Rich Proteoglycans (SLRPs), and they have all been implicated in regulating cancer progression.[67] Decorin is multifunctional and is likely to influence the tumor microenvironment via several mechanisms, including involvement in collagen organization and regulation of growth factor signaling.[64] Therefore, we investigated the expression of several matrix genes (including collagens, fibronectin, elastin, and lysyl oxidase (*Lox*)), transforming growth factor beta (*Tgfβ*) and downstream signaling factors, epidermal growth factor (*Egf*) and epidermal growth factor receptor (*Egfr*), and hepatocyte growth factor receptor (*Met*), as well as selected tumor markers (Supplementary Fig. 5). Decorin was co-expressed with several ECM-related genes, particularly the enzyme lysyl oxidase (Fig. 5F), and to some extent genes encoding collagens (Col8a1 and Col12a1; Fig. 5G and 5H). Lox is a secreted enzyme catalyzing collagen crosslinking and is known to promote metastatic spread of cancer by creating a fibrotic environment favorable to metastatic growth.[68] Decorin is also important for organization of collagen fibers and has been shown to be anti-fibrotic, in part via inactivation of TGFβ.[69] The mRNA expression pattern of *decorin* in cancer-associated fibroblasts (Fig. 5) and the co-localization with collagen 1A1 in the fibrous cap (Fig. 4B) may indicate a role for decorin in regulating fibrosis and matrix assembly in mammary tumors as well.

3.6. *Decorin decreases breast cancer cell proliferation in vitro*

To investigate whether decorin could reduce breast cancer cell proliferation, we treated the human breast cancer cell lines Michigan Cancer Foundation-7 (MCF-7 (a human breast cancer cell line with estrogen, progesterone, and glucocorticoid receptors[70]) and T47D (an appropriate experimental model to elucidate the progesterone-specific effects of a luminal A subtype of breast cancer[71]) with recombinant decorin *in vitro*. We showed that 10 nM recombinant decorin treatment markedly reduced both MCF-7 and T47D proliferation (Supplementary Fig. 6A and 6B). Moreover, T47D proliferation was also significantly decreased when treated with a lower dose (1 nM) of recombinant decorin (Supplementary Fig. 6B). These results suggest that decorin can reduce breast cancer cell proliferation, a result consistent with our observations that decorin can decrease tumor grade and increase survival in patients.

3.7. *Overexpression of decorin in skeletal muscle or treatment with recombinant decorin does not increase tumor decorin levels and does not affect breast cancer progression*

To this point, we had demonstrated that exercise training reduced tumor development in the MMTV-PyMT model, that decorin was a *bona fide* exercise-induced secretory factor which increases in breast cancer patients during acute exercise, that tumor decorin levels in patients with breast cancer was associated with a better prognosis, and that decorin decreases

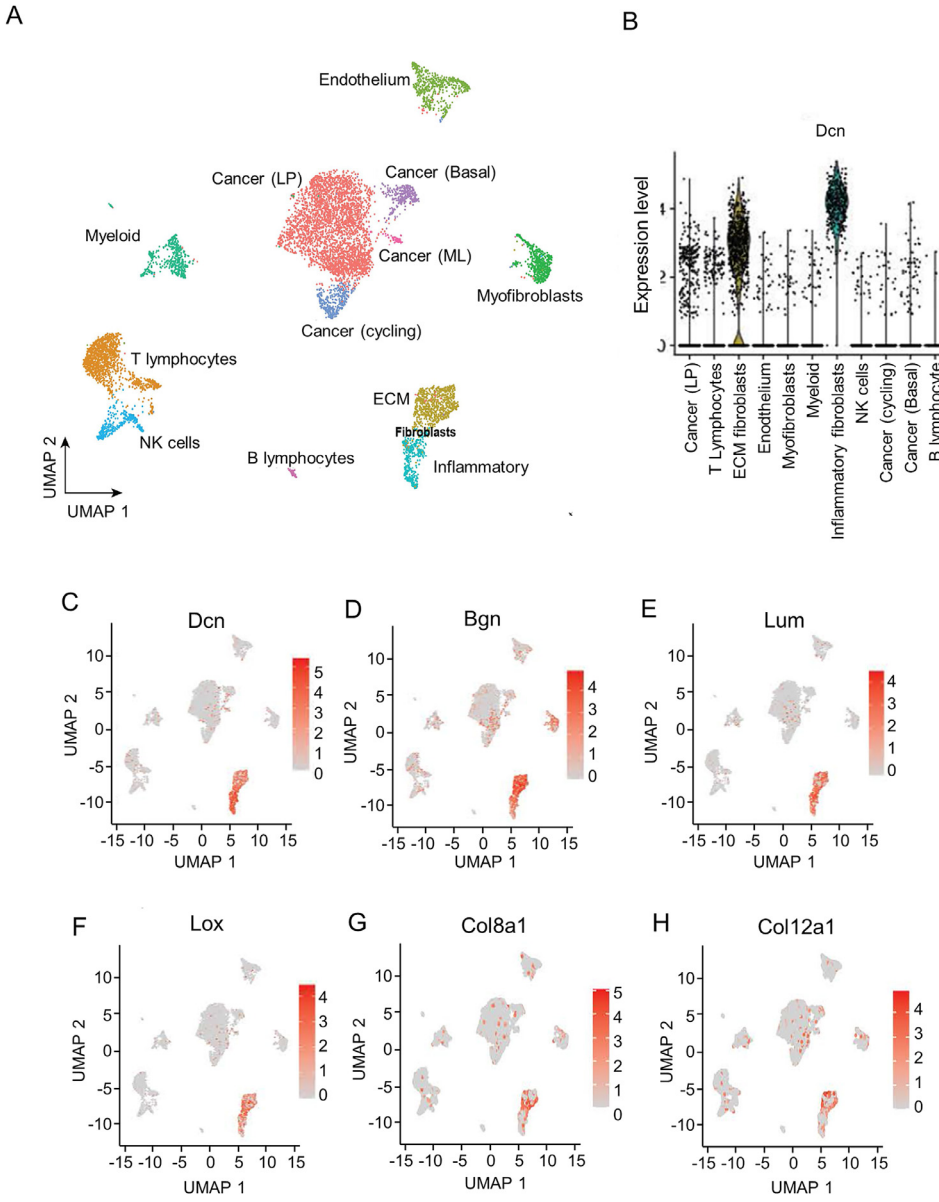

Fig. 5. Single-cell RNA sequencing of PyMT tumors. (A) Cell composition of MMTV-PyMT tumors. tSNE plot showing cell clusters defined by a k-means-based clustering algorithm. (B) Violin plot of the decorin mRNA expression in cell clusters defined in panel A. (C−H) mRNA expression of *Dcn, Bgn, Lum, Lox, Col8a1,* and *Col12a1* plotted in the tSNE defined in panel A. tSNE = t-distributed stochastic neighbor embedding. MMTV-PyMT = mammary specific polyoma-virus middle T antigen overexpression mouse model. Bgn = biglycan; Col = collagen; Dcn = decorin; ECM = extracellular matrix; Lox = lysyl oxidase; LP = luminal progenitor; Lum = lumican; ML = mature luminal; NK = natural killer; UMAP = uniform manifold approximation and projection.

breast cancer cell proliferation *in vitro*. This led us to hypothesize that decorin could be secreted from skeletal muscle during exercise to infiltrate the mammary tissue and arrest tumor development. To test this hypothesis, we performed muscle-specific decorin overexpression studies in the MMTV-PyMT model. We employed techniques using recombinant viral vectors derived from non-pathogenic adeno-associated viruses (rAAV). Specifically, rAAVs expressing FLAG-tagged decorin (AAV:Dcn) or empty vector control (AAV:Con) were injected in to 3 muscles of both hind limbs. We detected both decorin and FLAG in skeletal muscle of AAV:Dcn mice using immunohistochemistry (Fig. 6A). As a negative control for decorin, we used muscle from decorin-deficient ($Dcn^{-/-}$) animals. We also detected FLAG-tagged decorin in AAV:Dcn muscle by immunoprecipitation of FLAG coupled with immunoblotting for both FLAG and decorin (Fig. 6B). We were able to detect endogenous decorin in the muscles of the AAV:Con animals by immunohistochemistry (Fig. 6A). Notwithstanding, both decorin and FLAG were markedly increased in skeletal muscle of AAV:Dcn compared with AAV:Con, as measured by both techniques (Fig. 6A and 6B). This degree of decorin overexpression was sufficient to increase serum decorin approximately 2-fold as compared with AAV: Con mice (Fig. 6C). Despite the increase in serum decorin observed in the AAV:Dcn mice, this did not result in any increased protein expression in either the mammary or

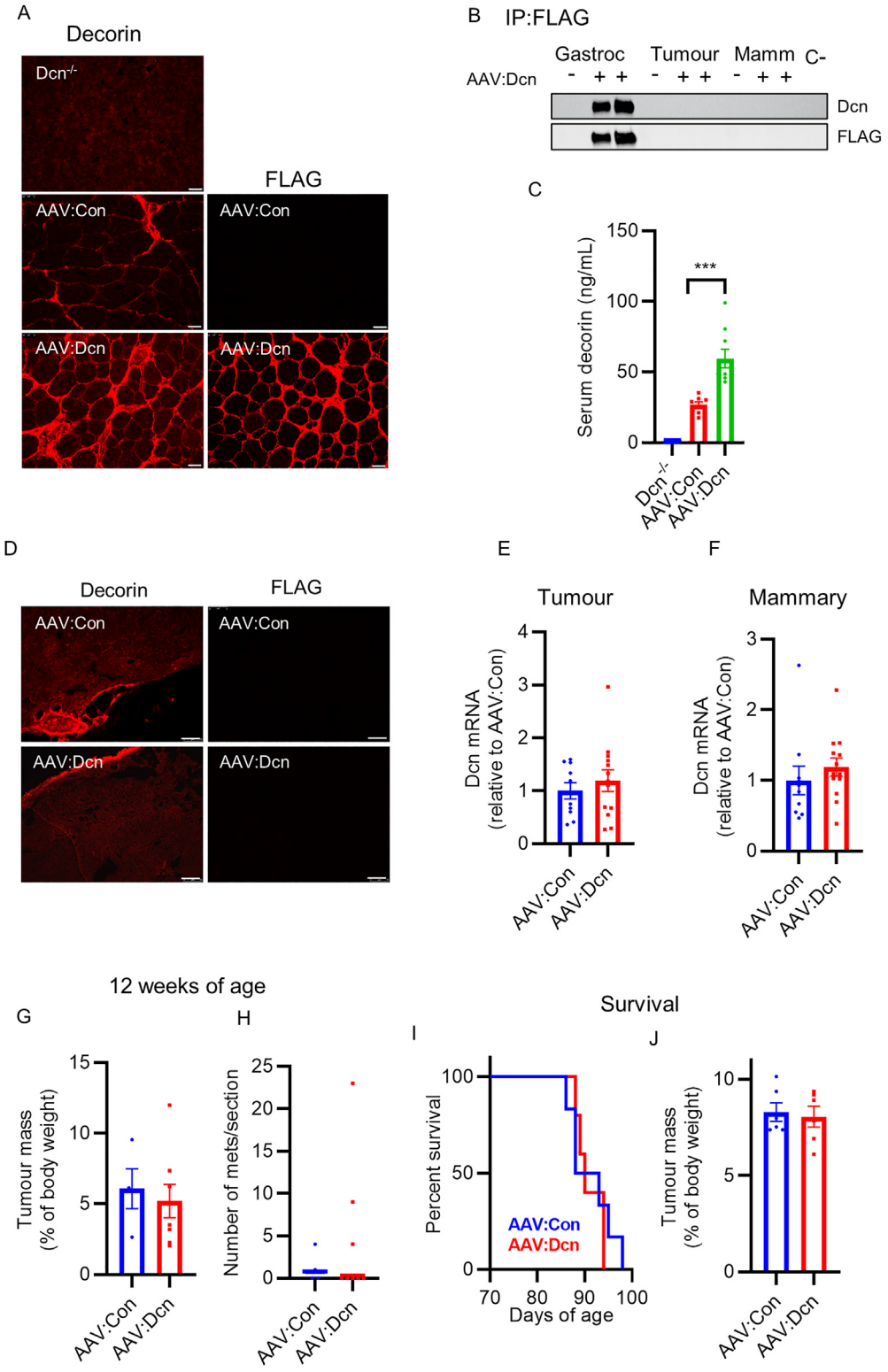

Fig. 6. Overexpression of decorin in skeletal muscle of MMTV-PyMT mice. Skeletal muscles were injected with recombinant AAVs carrying either FLAG-tagged decorin (AAV:Dcn) or an empty vector control (AVV:Con) at 6 weeks of age. (A) Immunoflourescence staining of decorin and FLAG in skeletal muscles of AAV:Dcn and AAV:Con mice. Muscles from decorin-deficient mice ($Dcn^{-/-}$) were used as negative controls for decorin staining. Scale bar represents 25 μm. (B) Immunoprecipitation of FLAG from lysates of gastrocnemius muscle, tumor tissue, and mammary fat pad in AAV:Con and AAV:Dcn mice; C- was a protei-free negative control. Immunoprecipitates were subjected to SDS-PAGE and immunoblotted for decorin or FLAG. (C) Decorin concentration in serum from $Dcn^{-/-}$, mice overexpressing decorin in skeletal muscle (AAV:Dcn), or control mice (AAV:Con). (D) Immunofluorescence staining of decorin and FLAG in tumors from AAV:Dcn and AAV:Con mice. Scale bar represents 75 μm. (E–F) Decorin mRNA expression in tumors and mammary fat pad. (G–H) At 12 weeks of age, tumor burden was measured as total tumor mass relative to body weight (%), and number of lung metastases was quantified as number of metastatic lesions per microtomy section. (I–J) Survival; animals were euthanized when tumor burden was 10% ± 3% or when the largest tumor was >1 cm^2. Days of age at termination (I) and tumor burden (J). Data expressed as means ± SEM (C, E, F, G, H, J). (n = 5–13 mice per group). *** $p < 0.001$. AAV = adeno-associated virus; Con = control; Dcn = decorin; MMTV-PyMT = mammary specific polyomavirus middle T antigen overexpression mouse model; SDS-PAGE = sodium dodecyl-sulfate polyacrylamide gel electrophoresis; SEM = standard error of the mean.

tumor tissue as measured by immunoblotting or immunohistochemistry (Fig. 6B and 6D) or mRNA expression as measured by reverse transcription polymerase chain reaction (RT-PCR) in either the tumor or mammary non-tumor tissue (Fig. 6E and 6F). Not surprisingly, therefore, muscle-specific decorin overexpression did not affect tumor mass, metastasis, or survival when compared with AAV: Con mice (Fig. 6G−6J).

Our results from the muscle overexpression study were surprising since plasma decorin was almost doubled when we overexpressed decorin in skeletal muscle (Fig. 5C), and previous studies have shown that MDA-231 tumor xenografts respond to the systemic delivery of decorin.[72] We, therefore, performed 2 additional experiments where we systemically delivered recombinant decorin to severe combined immunodeficient (SCID) mice with the MDA-MB-231-HM cells injected into their mammary pads. In the first (low dose) experiment, ∼14 days post tumor-cell inoculation, mice were IP injected with 100 μg of recombinant decorin or an equal volume of saline (Control) every second day for ∼2 weeks, as was previously done in several studies showing tumor burden decreases.[27,73,74] Such an intervention regime did not affect tumor volume or metastatic burden progression (Fig. 7A and 7B). We then measured both plasma and tumor decorin and found that neither was increased by the dosing regimen (Fig. 7C and 7D). We reasoned that our dosing regime was insufficient as neither plasma nor tumor decorin increased in this experiment. We, therefore, performed another (high dose) experiment where mice received ∼2.5 times the dose of the low-dose experiment daily rather than every other day. In addition, we commenced the treatment approximately 7 days after tumor-cell inoculation. Even though plasma decorin was higher using this protocol (Fig. 7G), the tumor decorin content was not increased (Fig. 7H) and, unsurprisingly, neither tumor volume (Fig. 7E) nor metastatic burden (Fig. 7F) was affected by recombinant decorin treatment.

We next tested whether systemic decorin administration influenced the expression of tumor marker genes (Supplementary Fig. 7) and proteins relevant to tumor progression and decorin-induced alterations in signaling pathways (Supplementary Fig. 8). We did not detect any significant changes in decorin (*Dcn*), Receptor tyrosine-protein kinase (*Errb2*), toll-like receptor 4 (*Tlr4*), tumor necrosis factor (*Tnf*), transforming related protein 53 (*Trp53*), or transforming growth factor beta 1 (*Tgfb1*) mRNA expression. Furthermore, administration of decorin did not influence the abundance of BAX, p53, TNF alpha, EGF receptor, and phosphorylated SMAD2/3 as measured with western blot.

Taken together, these data indicate that even though plasma decorin can be increased in mouse models of breast cancer, this does not necessarily result in increased tumor decorin content and protection from breast cancer progression.

4. Discussion

According to epidemiological studies, long-term physical activity is beneficial for both prevention and treatment of breast cancer.[3−6] There are also several preclinical studies reporting cancer-protective effects of exercise.[9] In our study using the MMTV-PyMT murine model of tumor development, we demonstrated a beneficial effect on mammary tumor growth but not on lung metastases. In a similar mouse model, wheel running attenuated mammary tumor growth at an early but not a late cancer stage.[75] Other studies have reported protective effects of exercise in xenograft[76] or allograft models.[77] The effects of exercise on metastatic spread in preclinical models are more unclear, with preclinical findings indicating that exercise does not significantly affect markers of cancer metastasis incidence or severity.[78−80] However, the considerable methodological variability observed across studies should be acknowledged, and the potential effects of exercise on the progression of metastases still need to be clarified.

Most importantly, even though mice ran the same distance whether they were dual- or single-housed, protection against tumor development was only observed when mice were dually housed. As discussed, mice prefer social contact when given the choice,[57] possibly because single housing mice makes them less capable of coping with external stressors than their group-housed counterparts,[58] resulting in higher levels of psychological stress.[59] We measured circulating corticosterone in both the single- and dual-housed mice but observed no difference between cohorts (Supplementary Fig. 3). Nonetheless, our data clearly points to the beneficial effect of exercise on delaying the progression of tumor development in this mouse model.

Regular physical activity may protect against breast cancer by influencing risk factors such as adiposity, low-grade inflammation, metabolic health, and sex hormones.[9] Indeed, in our study, fat mass was markedly reduced by access to running wheels (Fig. 1E). It is also possible, however, that protection is driven by recurring acute exercise responses because acute exercise leads to marked systemic adaptations that can have direct effects on tumor biology. This concept was demonstrated by Dethlefsen et al.[43] in a series of experiments with human exercise-conditioned serum. Incubation with serum taken after acute exercise, but not after long-term training, reduced the viability of breast cancer cells *in vitro*. Interestingly, this also led to reduced tumorigenesis after implantation in mice.

Several myokines are released into circulation in response to acute exercise. The most studied myokine is IL-6, which can increase several fold in plasma during exercise.[81] IL-6 is involved in metabolic regulation but might also influence tumor development. In a preclinical study by Pedersen et al.,[82] voluntary wheel running slowed tumor growth by 60% in mice. This was attributed to epinephrine and IL-6 dependent mobilization of natural killer (NK) cells. Lastly, Aoi and colleagues[19] demonstrated anti-tumorigenic effects of the myokine SPARC in a mouse model of colon cancer. Kanzleiter et al.[22] previously reported that decorin is secreted from skeletal muscle; they demonstrated that muscle cells secrete decorin *in vitro*, and that plasma decorin is increased after acute resistance exercise. This earlier study did not prove, however, that the contracting leg was responsible for

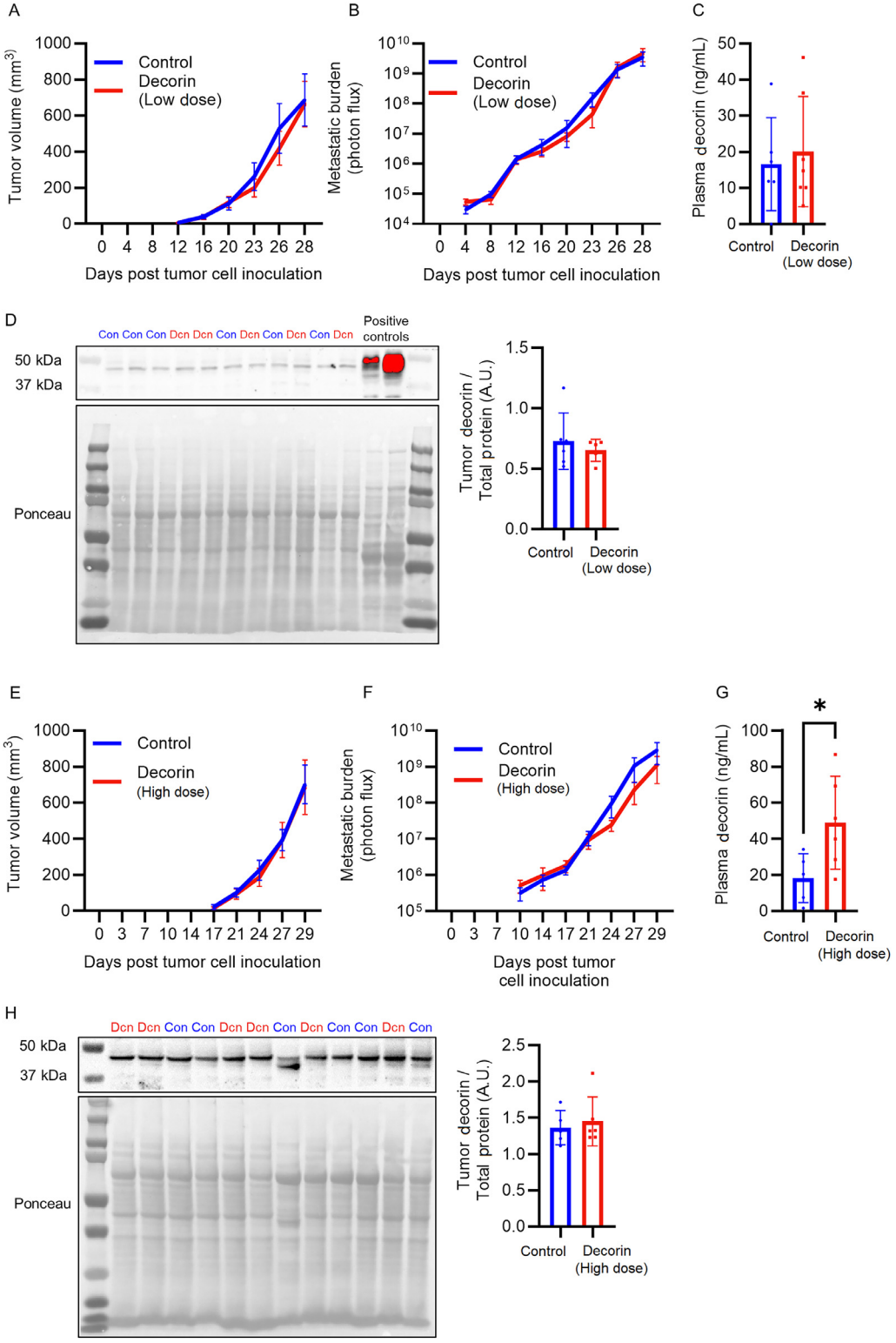

Fig. 7. Systemic delivery of recombinant decorin into SCID mice injected with MDA-MB-231-HM cells. SCID mice injected with the MDA-MB-231-HM cells into mammary pads received 2 different doses of recombinant decorin systemically. (A) Tumor volume, (B) metastatic burden, (C) plasma decorin levels, and (D) tumor decorin levels after the low-dose experiment. Mice were dosed every second day with 100 μg of recombinant decorin or an equal volume of saline (Control) ~14 days post tumor-cell inoculation. (E) Tumor volume, (F) metastatic burden, (G) plasma decorin levels, and (H) tumor decorin levels after the high-dose experiment. Mice were dosed daily with 10 mg/kg body weight (~2.5 times the dose of low-dose experiment) of recombinant decorin or an equal volume of saline (Control) ~7 days post tumor-cell inoculation. Tumor volume was assessed by calliper measurement of primary tumor growth and calculated as (length × width^2)/2. Metastatic burden was assessed by bioluminescence imaging detection. Plasma decorin levels were measured by ELISA. Tumor decorin levels were measured by western blot using total protein normalization. Two AAV:Dcn gastrocnemius lysates from the overexpression experiments were used as positive controls. Statistical testing was done with two-way analyses of variance or mixed effects model for repeated measures or Student's *t* test. Data expressed as means ± SEM. ($n = 5–7$ mice per group). A.U. = arbitrary unit; con = control; Dcn = decorin; ELISA = enzyme linked immunosorbent assay.

the increase in serum decorin in exercising humans.[22] In our study, we demonstrate that decorin is secreted from the contracting limb, and that it most likely comes from skeletal muscle. The abundance of decorin in both skeletal muscle and plasma was increased following acute exercise, even in women with breast cancer, and we detected a net release of decorin from the exercising leg in healthy human participants (Fig. 2).

Decorin is a ubiquitous proteoglycan located in extracellular matrices. Decorin can bind and "decorate" collagen fibers, which is of importance to collagen assembly, as decorin-deficient mice have abnormal collagen morphology and fragile skin.[83] The ability of decorin to bind to various growth factors or cell surface receptors allows it to influence several signal transduction pathways. For instance, decorin can inhibit TGFβ signaling by preventing it from binding to its receptor.[84] Decorin also interferes with several members of the receptor tyrosine kinase family, including EGF receptors (EGFR/ErbB1)[85] and hepatocyte growth factor receptor.[86] Decorin is, therefore, a multifunctional proteoglycan with the ability to influence a wide range of biological processes of relevance to tumor growth and metastatic spread, including proliferation, differentiation, migration, angiogenesis, autophagy, fibrosis, and inflammation.[25,26,64,87]

Several breast cancer xenograft studies have demonstrated cancer protection by intratumoral[29] delivery of decorin protein core or decorin overexpression by adenoviral transduction.[29,88] Reed et al.[29] reported a 70% decrease in tumor growth and a reduction in metastatic lesions by local treatment with either decorin or an adenoviral vector containing the decorin transgene. In another study, matrix metalloproteinase-8 (MMP-8) was found to suppress tumor growth and lung metastasis formation,[31] and subsequent mechanistic experiments indicated that this was due to MMP-8 mediated activation of decorin, which in turn led to reduced TGFβ signaling. Indeed, it is suggested that decorin core protein can act as a paracrine factor that modulates downstream signaling pathways. For instance, receptor tyrosine kinases on tumor cell membranes may be inhibited in a paracrine fashion by increased amounts of decorin in the ECM of stromal origin.[89]

In addition to the paracrine effects of decorin, several studies have reported systemic anti-tumorigenic effects. For example, tumor growth was inhibited when decorin was overexpressed at a distant site[28] or with systemic delivery.[72] In addition, Seidler et al.[27] reported reduced growth of an orthotopic squamous cell carcinoma xenograft in mice following IP injections of decorin. This was accompanied by accumulation of exogenous decorin in tumor tissue, downregulation of the EGF receptor, increased apoptosis, and a reduced mitotic index. Our hypothesis was, therefore, that exercise increases decorin release from the contracting limb, and if decorin can increase within the mammary tissue or tumor then the prognosis is enhanced. However, whether decorin can be released from the leg to enter the mammary tissue and protect against tumorigenesis thereby providing a molecular mechanism for the protective effects of exercise has not been addressed previously. Here, we did not observe effects on either primary tumor growth or formation of metastases when overexpressing decorin in the skeletal muscle, even though this resulted in increased circulating decorin (Fig. 6C). We also performed systemic injection studies, and the results were consistent with our muscle overexpression model in that, at least in our high-dose decorin experiment, plasma decorin was increased (Fig. 7G), but this was insufficient to decrease tumor volume or metastatic burden (Fig. 7E and 7F). One could argue that decorin has a short half-life[90] and, consequently, was degraded before a significant uptake by the tumor. However, we demonstrated in our high-dose experiments that decorin levels were still increased at the moment mice were sacrificed for blood collection (approximately 24 h from the last injection). Therefore, it is reasonable to suggest that decorin half-life is long enough to be available to the tumor.

We showed that decorin can reduce breast cancer cell proliferation when delivered to tumor cells *in vitro* (Supplementary Fig 6A and 6B). Considering this, the absence of changes in tumor volume or metastatic burden was likely due to the fact that, despite the increase in circulating decorin with muscle-specific overexpression or systemic injections, this was not sufficient to result in increased decorin in the tumor and mammary tissue (Figs. 6D−7F and 7H).

5. Strengths and limitations

The strengths of this study include the comprehensive preclinical and clinical models we have employed. We have demonstrated that exercise is protective in models of breast cancer but, critically, only when mice are not socially isolated. In addition, we have demonstrated that the proteoglycan decorin is a protein linked to breast cancer progression in humans that increases due to exercise in patients. Our data suggest that while decorin may be a therapeutic target to treat breast cancer progression when being injected into the tumor or fat pad to increase tumor decorin content, it is not a mechanism by which exercise exerts its progression. A major limitation to this conclusion is that the studies were performed exclusively in mice. It is important to note that Tralhão et al.[91] observed tumor growth inhibition even when decorin was overexpressed at a distant site. This suggests that in some models, elevated systemic delivery of decorin does confer protection. We also do not know what would happen to tumors in patient who have undergone exercise training, where systemic levels of decorin may increase. We are currently performing such studies. We cannot, therefore, totally dismiss a muscle-to-tumor decorin axis, although our existing data would argue against this hypothesis.

6. Conclusion

We have herein demonstrated that voluntary wheel running slows tumor progression in the transgenic polyoma middle T oncoprotein mouse model of luminal breast cancer (MMTV-PyMT), but only when mice are not caged alone. We have also shown that decorin is an exercise-induced muscle secretory

factor and a positive prognostic indicator of breast cancer progression in patients.

Authors' contributions

MH performed various experiments in mice (exercise and breast cancer development, and decorin overexpression), analyzed samples generated from human exercise studies, analyzed data and drafted the original manuscript; CLE performed experiments on mice (exercise studies, decorin overexpression and administration of recombinant decorin) and analyzed data; GDT performed experiments related to administration of recombinant decorin to mice and analyzed data; MP was involved in conceptualization and generation of preliminary data; DGO was involved with the mouse breast cancer model and generated the single cell sequencing data; OKF, EDM, and RDG performed experiments related to administration of recombinant decorin to mice; TGO and GEOM were involved in analysing data from human breast cancer datasets; ST and MSMM were involved in data analysis; JS generated proteomics data from decellularized tissues; EE performed experiments on mice; TEA was involved in production of recombinant decorin; MJM and MM were involved in LC/MS data acquisition; KIW, PG, and JFPW were involved in creating the AAV:Dcn overexpression model; HQ was involved in generating rAAV; TRC developed the method for proteomics analysis decellularized tissues and contributed with data in decorin; PH, JM, JFC, and MF were involved in exercise intervention studies in humans; RVI and EKS were involved in conceptualization and planning of the experiments with recombinant decorin; BGD performed experiments on cultured cells; MW was involved in conceptualization of the study, was responsible for the project administration and generated proteomics data from exercising mice; MAF acquired funding for the project, was involved in conceptualization of the study and wrote the original draft. All authors have read and approved the final version of the manuscript, and agree with the order of presentation of the authors.

Competing interests

MAF is a shareholder and scientific advisor for N-Gene Pharmaceuticals; MAF is the founder and shareholder of Celesta Therapeutics. All the support had no involvement in the study design and writing of the manuscript or the decision to submit it for publication. The authors declare that they have no other competing interests.

Data availability

Processed quantitative proteomics SILAC data are freely available at https://doi.org/10.25500/edata.bham.00001030.

Acknowledgments

The authors acknowledge the work of the staff at the animal research facilities at both the Garvan Institute of Medical Research and the Monash Institute of Pharmaceutical Sciences, Monash University. We also acknowledge the contribution of Erik Richter and Bente Keins from the Department of Nutrition, Exercise and Sports, University of Copenhagen for their help in obtaining blood samples from the human arteriovenous exercise study. MAF is a Senior Principal Research Fellow of the National Health and Medical Research Council of Australia (NHMRC) (APP1116936) and is also supported by an NHMRC Investigator Grant (APP1194141). Research in his laboratory was supported by project grants from the NHMRC (APP1042465, APP1041760, and APP1156511).

Supplementary materials

Supplementary materials associated with this article can be found in the online version at doi:10.1016/j.jshs.2024.100991.

References

1. Global Burden of Disease Cancer, Fitzmaurice C, Abate D, et al. Global, regional, and national cancer incidence, mortality, years of life lost, years lived with disability, and disability-adjusted life-years for 29 cancer groups, 1990 to 2017: A systematic analysis for the global burden of disease study. *JAMA Oncol* 2019;**5**:1749–68.
2. Jassem J, Buchanan M, Jänicke F, et al. The Hamburg statement: The partnership driving the European agenda on breast cancer. *Eur J Cancer* 2004;**40**:1810–1.
3. Kyu HH, Bachman VF, Alexander LT, et al. Physical activity and risk of breast cancer, colon cancer, diabetes, ischemic heart disease, and ischemic stroke events: Systematic review and dose–response meta-analysis for the global burden of disease study 2013. *BMJ* 2016;**354**:i3857. doi:10.1136/bmj.i3857.
4. Pizot C, Boniol M, Mullie P, et al. Physical activity, hormone replacement therapy and breast cancer risk: A meta-analysis of prospective studies. *Eur J Cancer* 2016;**52**:138–54.
5. Cormie P, Zopf EM, Zhang X, Schmitz KH. The impact of exercise on cancer mortality, recurrence, and treatment-related adverse effects. *Epidemiol Rev* 2017;**39**:71–92.
6. Spei ME, Samoli E, Bravi F, La Vecchia C, Bamia C, Benetou V. Physical activity in breast cancer survivors: A systematic review and meta-analysis on overall and breast cancer survival. *Breast* 2019;**44**:144–52.
7. Kohl HW, LaPorte R E, Blair SN. Physical activity and cancer. An epidemiological perspective. *Sports Med* 1988;**6**:222–37.
8. Rusch HP, Kline BE. The effect of exercise on the growth of a mouse tumor. *Cancer Res* 1944;**4**:116–8.
9. Hojman P, Gehl J, Christensen JF, Pedersen BK. Molecular mechanisms linking exercise to cancer prevention and treatment. *Cell Metab* 2018;**27**:10–21.
10. Kang DW, Lee J, Suh SH, Ligibel J, Courneya KS, Jeon JY. Effects of exercise on insulin, IGF axis, adipocytokines, and inflammatory markers in breast cancer survivors: A systematic review and meta-analysis. *Cancer Epidemiol Biomarkers Prev* 2017;**26**:355–65.
11. Goodwin PJ, Ennis M, Pritchard KI, et al. Insulin-like growth factor binding proteins 1 and 3 and breast cancer outcomes. *Breast Cancer Res Treat* 2002;**74**:65–76.
12. Tao MH, Shu XO, Ruan ZX, Gao YT, Zheng W. Association of overweight with breast cancer survival. *Am J Epidemiol* 2006;**163**:101–7.
13. Koelwyn GJ, Wennerberg E, Demaria S, Jones LW. Exercise in regulation of inflammation-immune axis function in cancer initiation and progression. *Oncology (Williston Park)* 2015;**29**:908–20.
14. Starkie RL, Rolland J, Angus DJ, Anderson MJ, Febbraio MA. Circulating monocytes are not the source of elevations in plasma IL-6 and TNF-alpha levels after prolonged running. *Am J Physiol Cell Physiol* 2001;**280**:C769–74.
15. Pedersen L, Idorn M, Olofsson G, et al. Voluntary running suppresses tumor growth through epinephrine- and IL-6-dependent NK cell mobilization and redistribution. *Cell Metab* 2016;**23**:554–62.

16. Zwirner NW, Domaica CI. Cytokine regulation of natural killer cell effector functions. *Biofactors* 2010;**36**:274–88.
17. Kurz E, Hirsch CA, Dalton T, et al. Exercise-induced engagement of the IL-15/IL-15Ralpha axis promotes anti-tumor immunity in pancreatic cancer. *Cancer Cell* 2022;**40**:720–37.
18. Cao L, Liu X, Lin EJ, et al. Environmental and genetic activation of a brain-adipocyte BDNF/leptin axis causes cancer remission and inhibition. *Cell* 2010;**142**:52–64.
19. Aoi W, Naito Y, Takagi T, et al. A novel myokine, secreted protein acidic and rich in cysteine (SPARC), suppresses colon tumorigenesis via regular exercise. *Gut* 2013;**62**:882–9.
20. Goh J, Niksirat N, Campbell KL. Exercise training and immune crosstalk in breast cancer microenvironment: Exploring the paradigms of exercise-induced immune modulation and exercise-induced myokines. *Am J Transl Res* 2014;**6**:422–38.
21. Gannon NP, Vaughan RA, Garcia-Smith R, Bisoffi M, Trujillo KA. Effects of the exercise-inducible myokine irisin on malignant and non-malignant breast epithelial cell behavior *in vitro*. *Int J Cancer* 2015;**136**:E197–202.
22. Kanzleiter T, Rath M, Görgens SW, et al. The myokine decorin is regulated by contraction and involved in muscle hypertrophy. *Biochem Biophys Res Commun* 2014;**450**:1089–94.
23. Danielson KG, Baribault H, Holmes DF, Graham H, Kadler KE, Iozzo RV. Targeted disruption of decorin leads to abnormal collagen fibril morphology and skin fragility. *J Cell Biol* 1997;**136**:729–43.
24. Järveläinen H, Sainio A, Wight TN. Pivotal role for decorin in angiogenesis. *Matrix Biol* 2015;**43**:15–26.
25. Zhang W, Ge Y, Cheng Q, Zhang Q, Fang L, Zheng J. Decorin is a pivotal effector in the extracellular matrix and tumour microenvironment. *Oncotarget* 2018;**9**:5480–91.
26. Buraschi S, Neill T, Iozzo RV. Decorin is a devouring proteoglycan: Remodeling of intracellular catabolism via autophagy and mitophagy. *Matrix Biol* 2019;**75**–**76**:260–70.
27. Seidler DG, Goldoni S, Agnew C, et al. Decorin protein core inhibits *in vivo* cancer growth and metabolism by hindering epidermal growth factor receptor function and triggering apoptosis via caspase-3 activation. *J Biol Chem* 2006;**281**:26408–18.
28. Tralhao J G, Schaefer L, Micegova M, et al. *In vivo* selective and distant killing of cancer cells using adenovirus-mediated decorin gene transfer. *FASEB J* 2003;**17**:464–6.
29. Reed CC, Waterhouse A, Kirby S, et al. Decorin prevents metastatic spreading of breast cancer. *Oncogene* 2005;**24**:1104–10.
30. Araki K, Wakabayashi H, Shintani K, et al. Decorin suppresses bone metastasis in a breast cancer cell line. *Oncology* 2009;**77**:92–9.
31. Soria-Valles C, Gutiérrez-Fernández A, Guiu M, et al. The anti-metastatic activity of collagenase-2 in breast cancer cells is mediated by a signaling pathway involving decorin and miR-21. *Oncogene* 2014;**33**:3054–63.
32. Desmedt C, Piette F, Loi S, et al. Strong time dependence of the 76-gene prognostic signature for node-negative breast cancer patients in the TRANSBIG multicenter independent validation series. *Clin Cancer Res* 2007;**13**:3207–14.
33. Ivshina AV, George J, Senko O, et al. Genetic reclassification of histologic grade delineates new clinical subtypes of breast cancer. *Cancer Res* 2006;**66**:10292–301.
34. Jönsson G, Staaf J, Vallon-Christersson J, et al. The retinoblastoma gene undergoes rearrangements in BRCA1-deficient basal-like breast cancer. *Cancer Res* 2012;**72**:4028–36.
35. Schmidt M, Böhm D, von Törne C, et al. The humoral immune system has a key prognostic impact in node-negative breast cancer. *Cancer Res* 2008;**68**:5405–13.
36. Dumas J, Gargano MA, Dancik GM. shinyGEO: A web-based application for analyzing gene expression omnibus datasets. *Bioinformatics* 2016;**32**:3679–81.
37. Mihály Z, Kormos M, Lánczky A, et al. A meta-analysis of gene expression-based biomarkers predicting outcome after tamoxifen treatment in breast cancer. *Breast Cancer Res Treat* 2013;**140**:219–32.
38. Wojtaszewski JFP, MacDonald C, Nielsen JN, et al. Regulation of 5′AMP-activated protein kinase activity and substrate utilization in exercising human skeletal muscle. *Am J Physiol Endocrinol Metab* 2003;**284**:E813–22.
39. Sjøberg KA, Frøsig C, Kjøbsted R, et al. Exercise increases human skeletal muscle insulin sensitivity via coordinated increases in microvascular perfusion and molecular signaling. *Diabetes* 2017;**66**:1501–10.
40. Jorfeldt L, Wahren J. Leg blood flow during exercise in man. *Clin Sci* 1971;**41**:459–73.
41. Whitham M, Parker BL, Friedrichsen M, et al. Extracellular vesicles provide a means for tissue crosstalk during exercise. *Cell Metab* 2018;**27**:237–51.
42. Midtgaard J, Christensen JF, Tolver A, et al. Efficacy of multimodal exercise-based rehabilitation on physical activity, cardiorespiratory fitness, and patient-reported outcomes in cancer survivors: A randomized, controlled trial. *Ann Oncol* 2013;**24**:2267–73.
43. Dethlefsen C, Lillelund C, Midtgaard J, et al. Exercise regulates breast cancer cell viability: Systemic training adaptations versus acute exercise responses. *Breast Cancer Res Treat* 2016;**159**:469–79.
44. Adamsen L, Quist M, Andersen C, et al. Effect of a multimodal high intensity exercise intervention in cancer patients undergoing chemotherapy: Randomised controlled trial. *BMJ* 2009;**339**:b3410. doi:10.1136/bmj.b3410.
45. Guy CT, Cardiff RD, Muller WJ. Induction of mammary tumors by expression of polyomavirus middle T oncogene: A transgenic mouse model for metastatic disease. *Mol Cell Biol* 1992;**12**:954–61.
46. Mayorca-Guiliani AE, Madsen CD, Cox TR, et al. ISDoT: *In situ* decellularization of tissues for high-resolution imaging and proteomic analysis of native extracellular matrix. *Nat Med* 2017;**23**:890–8.
47. Rappsilber J, Mann M, Ishihama Y. Protocol for micro-purification, enrichment, pre-fractionation and storage of peptides for proteomics using StageTips. *Nat Protoc* 2007;**2**:1896–906.
48. Winbanks CE, Chen JL, Qian H, et al. The bone morphogenetic protein axis is a positive regulator of skeletal muscle mass. *J Cell Biol* 2013;**203**:345–57.
49. Valdes-Mora F, Salomon R, Gloss B, et al. Single-cell RNAseq uncovers involution mimicry as an aberrant development pathway during breast cancer metastasis. *bioRxiv* 2019. doi:10.1101/624890.
50. Salomon R, Kaczorowski D, Valdes-Mora F, et al. Droplet-based single cell RNAseq tools: A practical guide. *Lab Chip* 2019;**19**:1706–27.
51. Macosko EZ, Basu A, Satija R, et al. Highly parallel genome-wide expression profiling of individual cells using nanoliter droplets. *Cell* 2015;**161**:1202–14.
52. Butler A, Hoffman P, Smibert P, Papalexi E, Satija R. Integrating single-cell transcriptomic data across different conditions, technologies, and species. *Nature Biotechnol* 2018;**36**:411–20.
53. Becht E, McInnes L, Healy J, et al. Dimensionality reduction for visualizing single-cell data using UMAP. *Nat Biotechnol* 2019;**37**:38–44.
54. Fisher LW, Stubbs JT, Young MF. Antisera and cDNA probes to human and certain animal model bone matrix noncollagenous proteins. *Acta Orthop Scand Suppl* 1995;**66**:61–5.
55. Drew BG, Hamidi H, Zhou Z, et al. Estrogen receptor (ER)α-regulated lipocalin 2 expression in adipose tissue links obesity with breast cancer progression. *J Biol Chem* 2015;**290**:5566–81.
56. Fantozzi A, Christofori G. Mouse models of breast cancer metastasis. *Breast Cancer Res* 2006;**8**:212. doi:10.1186/bcr1530.
57. Van Loo PL, Van de Weerd H A, Van Zutphen LF, Baumans V. Preference for social contact versus environmental enrichment in male laboratory mice. *Lab Anim* 2004;**38**:178–88.
58. Bartolomucci A, Palanza P, Sacerdote P, et al. Individual housing induces altered immuno-endocrine responses to psychological stress in male mice. *Psychoneuroendocrinology* 2003;**28**:540–58.
59. Kalliokoski O, Teilmann AC, Jacobsen KR, Abelson KS, Hau J. The lonely mouse-single housing affects serotonergic signaling integrity measured by 8-OH-DPAT-induced hypothermia in male mice. *PLoS One* 2014;**9**:e111065. doi:10.1371/journal.pone.0111065.
60. Liu N, Wang Y, An AY, Banker C, Qian YH, O'Donnell JM. Single-housing induced effects on cognitive impairment and deprtession-like behavious in male and female mice involve neuroplasticity-related signaling. *Eur J Neurosci* 2020;**52**:2694–704.

61. Kruger M, Moser M, Ussar S, et al. SILAC mouse for quantitative proteomics uncovers kindlin-3 as an essential factor for red blood cell function. *Cell* 2008;**134**:353–64.
62. Whitham M, Febbraio MA. The ever-expanding myokinome: Discovery challenges and therapeutic implications. *Nat Rev Drug Discov* 2016;**15**:719–29.
63. Whitham M, Parker BL, Friedrichsen M, et al. Extracellular vesicles provide a means for tissue crosstalk during exercise. *Cell Metab* 2018;**27**:237–51.
64. Sainio AO, Järveläinen HT. Decorin-mediated oncosuppression–A potential future adjuvant therapy for human epithelial cancers. *Br J Pharmacol* 2019;**176**:5–15.
65. Aoi W, Naito Y, Takagi T, et al. A novel myokine, secreted protein acidic and rich in cysteine (SPARC), suppresses colon tumorigenesis via regular exercise. *Gut* 2013;**62**:882–9.
66. Bartoschek M, Oskolkov N, Bocci M, et al. Spatially and functionally distinct subclasses of breast cancer-associated fibroblasts revealed by single cell RNA sequencing. *Nat Commun* 2018;**9**:5150. doi:10.1038/s41467-018-07582-3.
67. Appunni S, Anand V, Khandelwal M, Gupta N, Rubens M, Sharma A. Small leucine rich proteoglycans (decorin, biglycan and lumican) in cancer. *Clin Chim Acta* 2019;**491**:1–7.
68. Cox TR, Gartland A, Erler JT. Lysyl oxidase, a targetable secreted molecule involved in cancer metastasis. *Cancer Res* 2016;**76**:188–92.
69. Baghy K, Iozzo RV, Kovalszky I. Decorin-TGFβ axis in hepatic fibrosis and cirrhosis. *J Histochem Cytochem* 2012;**60**:262–8.
70. Horwitz KB, Costlow ME, McGuire WL. MCF-7: A human breast cancer cell line with estrogen, androgen, progesterone, and glucocorticoid receptors. *Steroids* 1975;**26**:785–95.
71. Yu S, Kim T, Yoo KH, Kang K. The T47D cell line is an ideal experimental model to elucidate the progesterone-specific effects of a luminal A subtype of breast cancer. *Biochem Biophys Res Commun* 2017;**486**:752–8.
72. Buraschi S, Neill T, Owens RT, et al. Decorin protein core affects the global gene expression profile of the tumor microenvironment in a triple-negative orthotopic breast carcinoma xenograft model. *PLoS One* 2012;**7**:e45559. doi:10.1371/journal.pone.0045559.
73. Mondal DK, Xie C, Pascal GJ, Buraschi S, Iozzo RV. Decorin suppresses tumor lymphangiogenesis: A mechanism to curtail cancer progression. *Proc Natl Acad Sci U S A* 2024;**121**:e2317760121. doi:10.1073/pnas.2317760121.
74. Goldoni S, Seidler DG, Heath J, et al. An antimetastatic role for decorin in breast cancer. *Am J Pathol* 2008;**173**:844–55.
75. Goh J, Tsai J, Bammler TK, Farin FM, Endicott E, Ladiges WC. Exercise training in transgenic mice is associated with attenuation of early breast cancer growth in a dose-dependent manner. *PLoS One* 2013;**8**:e80123. doi:10.1371/journal.pone.0080123.
76. Dethlefsen C, Hansen LS, Lillelund C, et al. Exercise-induced catecholamines activate the hippo tumor suppressor pathway to reduce risks of breast cancer development. *Cancer Res* 2017;**77**:4894–904.
77. Betof AS, Lascola CD, Weitzel D, et al. Modulation of murine breast tumor vascularity, hypoxia, and chemotherapeutic response by exercise. *J Natl Cancer Inst* 2015;**107**:djv040. doi:10.1093/jnci/djv040.
78. Smeda M, Przyborowski K, Proniewski B, et al. Breast cancer pulmonary metastasis is increased in mice undertaking spontaneous physical training in the running wheel: A call for revising beneficial effects of exercise on cancer progression. *Am J Cancer Res* 2017;**7**:1926–36.
79. Rincon-Castanedo C, Morales JS, Martín-Ruiz A, et al. Physical exercise effects on metastasis: A systematic review and meta-analysis in animal cancer models. *Cancer Metastasis Rev* 2020;**39**:91–114.
80. Ashcraft K A, Peace RM, Betof AS, Dewhirst MW, Jones LW. Efficacy and mechanisms of aerobic exercise on cancer initiation, progression, and metastasis: A critical systematic review of *in vivo* preclinical data. *Cancer Res* 2016;**76**:4032–50.
81. Pal M, Febbraio MA, Whitham M. From cytokine to myokine: The emerging role of interleukin-6 in metabolic regulation. *Immunol Cell Biol* 2014;**92**:331–9.
82. Pedersen L, Idorn M, Olofsson GH, et al. Voluntary running suppresses tumor growth through epinephrine-and IL-6-dependent NK cell mobilization and redistribution. *Cell Metab* 2016;**23**:554–62.
83. Danielson KG, Baribault H, Holmes DF, Graham H, Kadler KE, Iozzo RV. Targeted disruption of decorin leads to abnormal collagen fibril morphology and skin fragility. *J Cell Biol* 1997;**136**:729–43.
84. Yamaguchi Y, Mann DM, Ruoslahti E. Negative regulation of transforming growth factor-β by the proteoglycan decorin. *Nature* 1990;**346**:281–4.
85. Santra M, Reed CC, Iozzo RV. Decorin binds to a narrow region of the epidermal growth factor (EGF) receptor, partially overlapping but distinct from the EGF-binding epitope. *J Biol Chem* 2002;**277**:35671–81.
86. Goldoni S, Humphries A, Nyström A, et al. Decorin is a novel antagonistic ligand of the Met receptor. *J Cell Biol* 2009;**185**:743–54.
87. Järvinen TAH, Ruoslahti E. Generation of a multi-functional, target organ-specific, anti-fibrotic molecule by molecular engineering of the extracellular matrix protein, decorin. *Br J Pharmacol* 2019;**176**:16–25.
88. Oh E, Choi IK, Hong J, CO Yun. Oncolytic adenovirus coexpressing interleukin-12 and decorin overcomes Treg-mediated immunosuppression inducing potent antitumor effects in a weakly immunogenic tumor model. *Oncotarget* 2017;**8**:4730–46.
89. Rigoglio NN, Rabelo ACS, Borghesi J, et al. The tumor microenvironment: Focus on extracellular matrix. *Adv Exp Med Biol* 2020;**1245**:1–38.
90. Geyik A, Koc B, Micili SC, Kiray M, Vayvada H, Guler S. Effect of decorin protein administration on rat sciatic nerve injury: An experimental study. *Neurol Res* 2022;**44**:252–61.
91. Tralhão JG, Schaefer L, Micegova M, et al. *In vivo* selective and distant killing of cancer cells using adenovirus-mediated decorin gene transfer. *FASEB J* 2003;**17**:464–6.